Advanced Course on Tissue Remodeling
ACTR'04 – (pp.241–300) – Warsaw, 2004.

Introduction to Remodeling of Arteries

Alexander Rachev

Georgia Institute of Technology
315 Ferst Drive, IBB Building
Atlanta, GA, 30332
On leave from the Institute of Mechanics
Bulgarian Academy of Sciences
alexander.rachev@me.gatech.edu

When soft biological tissues are exposed to long-lasting alterations in their mechanical environment, the resultant changes are in shape, structure and/or mechanical properties. The response might be associated with mass creation and resorption and is termed *remodeling*. This article provides a review of the main experimental findings on remodeling of arteries, for which this phenomenon is well studied. Few theoretical investigations on arterial remodeling that use models in terms of continuum mechanics are considered. Finally, some studies on remodeling-related problems associated with the use and fabrication of arterial grafts are presented.

Key words: *growth, remodeling, non-linear solid mechanics, artery, vascular grafts*

1. Introduction

Living organisms of mammalians consist of hard biological tissues such as bone and teeth, soft tissues such as vascular tissue, skeletal muscle, tendons, heart muscle, skin, and biological fluids such as blood, lymph, and synovial fluid. Soft biological tissues consist of cells and extracellular matrix produced by smooth muscles and fibroblast cells. The matrix consists of connective tissues such as elastin and collagen and ground substances. The cell type, quantity, and the composition of the extracellular matrix depend on tissue type and spatial localization within the organ or tissue. The structure of soft tissue alters during development and aging and due to the progression of certain diseases.

Soft tissues build organs or structures of specific biological function. In some of them mechanics plays a significant role. For instance, large arteries are tubes that transport blood from the heart to tissues and organs and supply them with nutrition and oxygen. Due to their elastic properties arteries transform the highly pulsatile heart output into a flow of moderate fluctuations. The heart serves as a pump to maintain the blood circulation. Muscles generate force, which is transmitted by tendons to bones, etc.

This article focuses on the mechanics and remodeling of arterial vessels. Arterial diseases are the leading cause of death in most countries. Therefore arterial biomechanics, and in particular the processes of remodeling and adaptation, are more thoroughly studied in comparison to other soft tissues.

Arteries exhibit a layered structure (Fig. 1). Endothelial cells (ECs) form one-cell-thick layer, which together with the underlying membrane is called the *intima* and is in direct contact with the flowing blood. The thickest layer, called the *media*, is the major load-bearing structure. It consists of smooth muscle cells (SMCs), collagen fibers, elastin and ground substance matrix. In most large arteries SMCs align mainly in the circumferential direction. The *adventitia* is the outermost layer and consists of collagen fibers, ground substance and some fibroblasts.

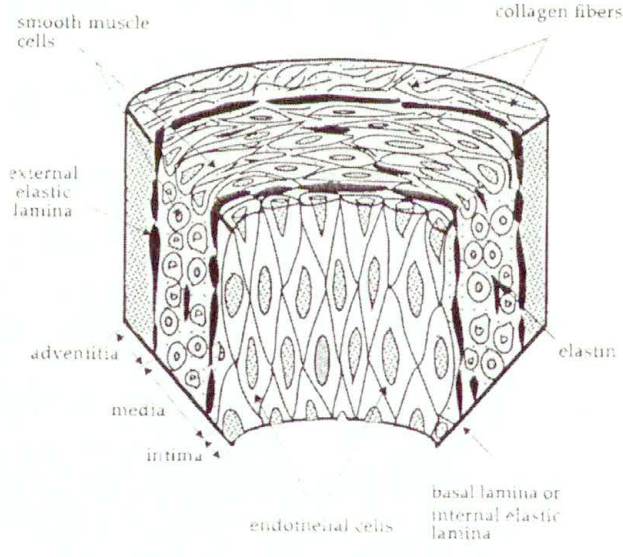

FIGURE 1. Schematic representation of the structure and composition of an artery (with the kind permission of H. Achakri).

The ratios between the collagen, the elastin, and the ground substances vary with location along the arterial tree. In a healthy matured artery, the cell production (mitosis) and cell death (apoptosis), as well as the extracellular matrix synthesis and degradation are slow and balanced processes. Therefore, they result in maintenance of arterial geometry, structure and composition. During development, aging and progression of some diseases the aforementioned processes may progress differently and may cause an increase or decrease in the arterial mass and/or alteration of the composition and organization of the vascular tissue.

From a mechanical point of view, soft tissues bear loads and/or generate and transmit forces. Arteries are subjected to axial forces due to surrounding tissues; to a periodic arterial pressure, which change from a diastolic to systolic value; and to flow-induced shear forces applied at the inner surface due to friction between the arterial wall and the blood. The load varies during development, maturity, and aging. Moreover, pressure and blood flow might transiently change during some physiological states. For instance, physical exercises are accompanied by an increase in pressure and an increase in cardiac output. Finally, changes in the mechanical environment are typical for some pathological states. *Hypertension* is characterized by a chronic increase in pressure. *Arteriosclerosis* leads to narrowing of the arterial lumen *(stenosis)* that causes a reduction or even total arrest of blood flow downstream of a stenosis.

Response of vascular tissue to applied loads depends on the state of the cellular components. When the viability of the SMCs is not preserved under experimental conditions, an artery manifests the *passive mechanical response.* Results from uniaxial tests on strips or from inflation and extension of arterial segments excised from the organism (*in vitro* experiments) have shown that the arterial tissue exhibits complex mechanical properties. The material undergoes large deformations, manifests pronounced physical non-linearity and mechanical anisotropy, and is practically incompressible. The passive response occurs instantaneously after the load is applied and is not very sensitive to the strain rate, though the tissue manifests hysteresis, relaxation and creep showing features of viscoelasticity. Under physiological loads, however, the passive mechanical properties are reasonably described by considering the arterial tissue as a non-linear elastic solid. The stress-strain constitutive equations follow from a strain energy density function that depends on the components of the finite strain tensor. In the general case, the strain energy

function is determined from data of at least two-dimensional experiments. At the microlevel the passive mechanical properties are due to the deformation and orientation of long chained protein molecules and to the interaction between tissue constituents.

When the viability of the SMCs is preserved and they are appropriately stimulated, the SMCs can contract or relax resulting in changes in the arterial diameter and wall thickness. The artery manifests the *active mechanical response* having a characteristic time of several seconds or minutes. Under normal physiological conditions, the SMCs are partially contracted and form the *basal muscular tone*, which reflects the basal value of the SMCs activation. Substances such as KCl and norepinephrine are used to evoke an active response when arteries are investigated at *in vitro* conditions. As stimuli for initiating smooth muscle contraction *in vivo* might serve local mechanical quantities such as strain or stress. An increase in the circumferential wall stress causes contraction of the SMCs, which leads to a constriction of the artery. This reaction is called the *myogenic response* or *Bayliss effect* and is independent of ECs. Muscle contraction can develop at constant length (*isometric contraction*) under constant tension (*isotonic contraction*) or at constant pressure (*isobaric contraction*). At the micro level, the muscle contraction includes a series of coupled mechanical, electrical and chemical processes in which the intercellular concentration of free calcium ions (Ca^{++}) plays a key role.

In contrast to the vast results on mathematical description of the passive behavior of the vascular tissue, the constitutive formulation that takes into account the muscular contraction is still fragmentarily studied. Most of the models proposed so far are based on the assumption that the total stress in the stimulated arterial wall is a sum of an active and passive stress. The passive stress is the stress borne by the passive structural components of the arterial wall, i.e. the elastin and the collagen. The active stress is the stress generated by the smooth muscle cells when they are stimulated. It is assumed that the passive stress in a constricted artery is equal to the passive stress in a fully relaxed artery, both compared at equivalent strain. This hypothesis is adopted in Hill's functional model shown in Fig. 2. The tissue consists of a parallel elastic element (PE), a serial elastic element (SE) and a contractile element (CE), [1]. The CE freely deforms when SMCs are relaxed and only the PE element deforms and generates a passive force. When the muscle is stimulated to contract the CE element shortens and

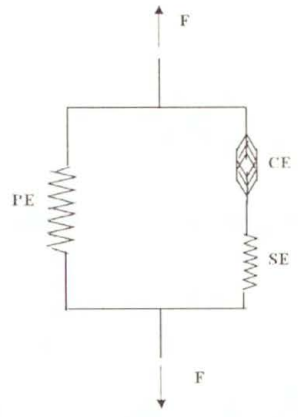

FIGURE 2. Schematics of Hill's model of the muscle contraction

the SE elements elongates producing an active tension. Hill's model gives one probable mechanism for development of an active arterial response. It is possible, however, that a contraction of the vascular smooth muscle not only generates an active tension but also causes a rearrangement of the passive structural components. Then the contribution of the non-cellular components in the load bearing, which is described in terms of a passive stress is different compared to the case when the muscle is relaxed.

Both the passive and the active mechanical response manifest without a change in tissue mass and structure. Experiments in living tissues have shown that mechanical environment can cause mass creation or resorption and/or lead to rearrangement of the structural constituents. As a result the organ or the structure that is built-up by the soft tissue might change its geometry and mechanical response. This behavior is called *remodeling*. As a rule remodeling occurs as a long-term response when changes in the mechanical environments persist for at least few days and weeks or sometimes months.

Irreversible changes in the arterial geometry and structure occur also during the period of development and maturation and the process is termed as *growth*. The growth of arteries is determined by two groups of factors. Firstly, those of genetic origin, which may include vessel size and topology, the rate of maturity and ageing, and any inherited tendency towards developing occlusive and degenerative diseases. Secondly, the growth is modulated by the epigenetic factors including the age-related changes in the mechanical environment experienced by the arterial wall. Some authors term the processes

of mass change as growth, property change as remodeling and shape change as morphogenesis [2, 3]. In this article remodeling is used for description of any alteration in tissue mass and mechanical properties caused by the mechanical factors. On the micro level, the remodeling is due to several factors: i) the change of cell number caused by unbalanced replication (proliferation or hyperplasia) and cell death (apoptosis or necrosis); ii) to change in cell size (hypertrophy); iii) to migration of cells; iv) to unbalance between extracellular matrix synthesis and degradation. These processes involve interaction of multiple ionic and enzymic pathways, whose precise nature remains unknown.

At the macro level, remodeling appears as changes in the geometrical dimensions and mechanical response of the artery, which do not result from the deformation caused by the altered loads. Sometimes geometrical and mechanical alterations are accompanied by changes in wall structure and composition. Moreover, remodeling may lead to changes in the arterial response when arterial smooth muscle cells are stimulated to relax or contract. Because arteries are permanently subjected to loads, remodeling also affects the strain and stress fields in the arterial wall.

The first studies on the influence of the mechanical environment on living tissues date back to the nineteenth century. In 1869 Wolff formulated his famous law, which states that there exists a strong interrelation between the structure of a bone and the stress field caused by the loading to which the bone is subjected. Later Roux [4] introduced the concept of the functional adaptation of bone to applied load. For soft tissues, in particular blood vessels, Thoma [5], on the basis of studies of blood vessels in the embryonic chick, concluded that mechanical forces play an important role in the modification of the vascular structure. However, intensive biomechanical investigations on arterial remodeling were not carried out until recent years. The phenomena of growth and remodeling in bones and soft tissues related to stress fields were discussed by Fung in his book *Biomechanics. Motion, Flow, Stress, and Growth* [6]. Results from many experimental investigations and continuum mechanics-based models of growth, remodeling and morphogenesis of living systems can be find in the review article [2] and in the monographs *Mechanics of growth and morphogenesis* [7] and *Cardiovascular Solid Mechanics* [3].

The objective of this article is to provide the reader with some introductory information and main trends in experimental and theoretical investigations on remodeling of arteries. The paper focuses on macro-level effects

that follow changes in arterial pressure, blood flow or local disturbances in the mechanical environment of an artery. Several studies in which the author has been involved are used to illustrate mathematical modeling in terms of continuum mechanics.

2. Review of Some Experimental Investigations on Arterial Wall Remodeling

In general, experimental biomechanical investigations aim to answer *what*-type questions, such as *what are the effects of certain mechanical factors on the function and/or structure of a given organ.* In particular, experimental studies on remodeling of arteries address the following questions: i) how do the geometry and mechanical properties of arteries change in response to alteration in the mechanical environment? ii) which mechanical parameters might be associated with the remodeling as triggers or driving stimuli of the remodeling process?

Three approaches have been mainly used to study experimentally the effects of changes in mechanical environment on arteries: i) in vivo investigations; ii) investigations in organ culture systems; and iii) investigations in cell culture.

2.1. In vivo Studies

In general, *in vivo* investigations include experiments realizing controlled changes in the mechanical environment and data analysis using appropriate mathematical models. The *pure remodeling* of the arteries is assessed when geometrical dimensions are measured and compared in the state of zero-stress to eliminate the contribution of the passive elastic deformation. It is accepted that the zero-stress configuration appears when a ring segment of an artery free of external loads is cut radially. Then the artery springs open and the cross-section takes the form close to a circular sector characterized by an *opening angle* (see Appendix A, Fig. 20). This demonstrates the existence of residual strains and stresses in the arterial wall in the state of no load. Because arteries exhibit a basal tone that might affect the zero-stress configuration, [8], dimensions of remodeled and control vessels must be compared under equivalent conditions of smooth muscle activation, for instance at the state of maximally relaxed smooth muscle cells.

When geometrical dimensions are measured and compared under load conditions, this allows for evaluation of the *observed changes due to remo-*

deling. They result not only from remodeling process but also include the effects of the altered passive elastic deformation and altered contractile state of the vascular smooth muscle caused by the changes in the mechanical environment.

In this section, we give a brief review of some results from *in vivo* studies on arterial remodeling.

2.1.1. Remodeling in response to sustained changes in blood flow. Compensatory enlargement of arteries in response to increased flow has been demonstrated in animal models and human vessels. Kamiya and Togawa [9] showed that an arterio-venous fistula between the canine common carotid artery and the external jugular vein causes increased flow rate in one portion of the artery and decreased flow rate in another. The intervention creates a marked alteration in the flow-induced shear stress at the intima. Over time, however, the deformed inner arterial radius varies and its cube tends to become proportional to the blood flow rate. Assuming that blood is a Newtonian fluid and the blood flow represents a developed Poiseuille flow, the mean shear stress at the inner surface is

$$\tau = \frac{4\eta Q}{\pi r_i^3}, \tag{2.1}$$

where Q is the mean blood flow rate, r_i is the deformed inner radius and η is blood viscosity. Therefore, the remodeling results in restoring the mean shear stress to its baseline value, which is about 1.5 Pa. Similar results have been observed by other authors [10–12]. Figure 3 shows the decrease in diameter of the left common carotid artery of mature rabbits after left external carotid ligation, which reduces the blood flow by 70%. Compensatory enlargement in response to increased flow was also recorded during normal development and hypertension.

Although the blood flow rate changes throughout the arterial system, arteries adjust their diameter so as to maintain a constant flow-induced shear stress. The uniform shear stress distribution has been recorded experimentally in matured animals, [13–14], and during embryonic development [15]. Theoretically, the uniform shear stress has been derived from the Poiseuille law (Eq. (2.1)) and an optimization principle known as Murray's law, which states that the total energy required to drive the blood and the energy consumed by the vessel metabolism is minimum [16].

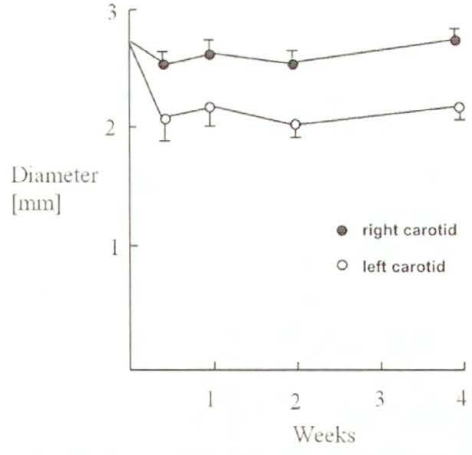

FIGURE 3. Diameter of left and right common carotid arteries after left external carotid legation (from [10])

More detailed analysis of the arterial response to an increase in flow rate shows that it involves two successive phases. Firstly, an acute increase in arterial lumen occurs, resulting from the temporary dilatation of the artery. This process is mediated by the endothelium through the release of substances such as endothelium-derived relaxing factor (EDRF), the principal component of which, nitric oxide (NO), causes relaxation of the smooth muscle cells. The acute vasomotor response is followed by a long-term reconstruction of the media due to proliferation and migration of the smooth muscle cells in such a way that the undeformed lumen of the vessel increases. Arterial enlargement causes an increase in wall tension and thereby increases the average circumferential stress. A compensatory thickening of the arterial wall was observed experimentally, which seems to restore the normal values of the wall stress [17].

Reduced flow elicits a different response. Again, it comprises two successive processes, but, in general, remodeling does not follow a time course that is simply the reverse of that observed under increased flow conditions. At first, the decrease in the wall shear stress sensed by the endothelium evokes a smooth muscle contraction leading to a constriction of the artery. Reductions in the release of EDRF or changes in concentration of specific vasoconstrictors are candidates as mediators of that process. Sustained decrease in flow provokes further processes, which occur mainly in the intima and result in wall thickening. Normally, remodeling is a self-limiting process and leads to a restoration of the baseline value of the wall shear stress. Smooth

muscle cells migrate into the intima and produce matrix proteins, resulting in a structure that resembles the underlying media. This new tissue is referred to as *fibrocellular intimal hypertrophy* [18]. Sometimes the remodeling does not lead to a configuration that maintains the normal level of the wall shear stress. The proliferation process might continue and ultimately leads to formation of a stenosis or obliteration of the lumen. The grown tissue is matrix-free, poorly organized and forms the *intimal hyperplasia* [18]. The exact mechanisms involved in the different modes of remodeling in response to changes in blood flow remain unclear.

Changes in flow cause remodeling of endothelial cells in the intima. It manifests as loss of cells when the flow is decreased and cell proliferation when the flow is increased. As a result, the surface density of the endothelial cells is maintained constant despite the changes in the arterial diameter resulting from remodeling of the media [12].

When an artery is denuded of intima, i.e. the endothelial cells are removed, a change in flow does not cause either acute vasomotor response or wall remodeling [12, 17]. Hence, the shear deformation of the endothelial cells appears to be the first in the chain of events that cause a change in the smooth muscle tone and succeeding remodeling of the wall.

The mechanisms by which arteries adapt to chronic blood flow alterations are different in young and mature animals. It was found that carotid arteries of adult rabbits subjected to reduced blood flow exhibit a decreased internal diameter and an increased wall thickness, but no significant changes in vessel mass and wall constituents were observed [12, 19]. Similarly, it was shown that remodeling in response to elevated blood flow ultimately produces a vessel that has composition and mechanical properties similar to the control artery [20, 21]. However, in young animals flow-induced remodeling results not only in a change in the geometrical dimensions but it also affects the wall structure and composition, disturbing the normal process of development and maturity [10].

2.1.2. Remodeling in response to sustained hypertension. Hypertension is a state of persistent increase in blood pressure. Though a slow elevation of pressure is a normal tendency accompanying ageing, a more severe increase in pressure is one of the major risk factors associated with the development of many cardiovascular diseases. Liu and Fung [22] and Fung and Liu [23] have studied the relationship between hypertension, hypertro-

phy, and the opening angle of the zero-stress state of arteries following an aortic constriction of a rat aorta. Banding of the abdominal aorta by a metal clip causes a persistent increase in the arterial pressure. The authors reported that the inner arterial radius remains practically constant. Because blood flow was not significantly changed, this means that the flow-induced shear at the endothelium maintains its baseline value. The wall thickness increased rapidly in the first few days after the onset of hypertension and then gradually attains a new homeostatic value (Fig. 4a). The time course of the opening angle exhibits a biphasic pattern (Fig. 4b). The fast increase in opening angle is followed by a slow decrease to an asymptotic value.

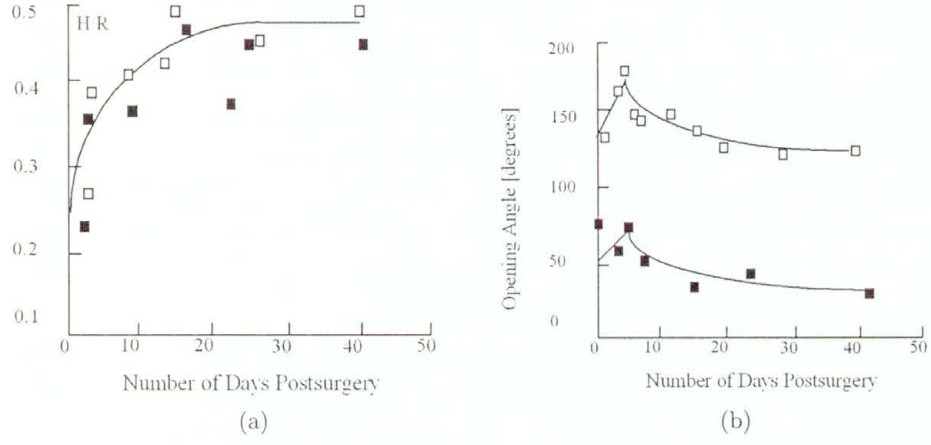

FIGURE 4. Time course of (a) wall thickness-mean radius ratio and (b) opening angle along the aorta at locations close to aortic root (□), and close to aorto-iliac bifurcation (■) (from [22])

Geometrical dimensions and applied loads are the only physical values that can be directly measured. In order to associate the recorded changes in arterial geometry with quantities that describe the stress and strain state in the arterial wall, it is necessary to adopt assumptions about geometry, loading and deformation of the vessel. An adequate stress analysis of soft tissue can be performed using the theory of finite elastic deformations [24]. Considering blood vessel as a circular cylindrical tube the mean circumferential stress in the arterial wall is calculated by the formula, often called the law of Laplace

$$\bar{\sigma}_\theta = \frac{Pr_i}{h}, \tag{2.2}$$

where P is the mean arterial pressure, r_i is the deformed inner radius, and h is the deformed wall thickness.

It was found that after hypertension-induced remodeling is complete, the circumferential stress in the hypertensive aorta is equal to the stress in the normotensive vessel indicating that the vessel thickens to restore the a baseline value of mean circumferential stress. This value is approximately 100 kPa [3]. Similar findings were reported by Vaishnav et al., [25], and by Matsumoto and Hayashi, [26], who used renal constriction to cause sustained hypertension.

In general, the changes in the opening angle combined with the changes in thickness tend to restore the circumferential stress distribution as it exists in the normotensive artery [8].

Pressure-induced remodeling of the mechanical properties is a much slower process than remodeling of the geometrical dimensions. It was found that after a relatively long period (16 weeks) the incremental elastic modulus of the aortic tissue in hypertensive rats is almost equal to the modulus calculated for normotensive animals [26, 27]. The incremental modulus characterizes the linearized relationship between the circumferential stress and the circumferential strain at the physiological deformed state. These findings was interpreted as a mechanical adaptation that tends to restore the normal arterial function under sustained hypertension.

Matsumoto and Hayashi [26] investigated also the histology of the aortic wall of control and hypertensive rats. They found that the thickening, which occurs mainly in the media, is due to the smooth muscle hypertrophy and an increase in ground substances produced by the SMCs. The authors showed that these effects are most pronounced in the inner lamellar units of the media. Because elevated pressure causes a greater increase in the circumferential stress at the inner portion of the wall thickness (see Appendix A) these findings support the hypothesis that remodeling is induced and "driven" by the wall stress. Moreover, the non-uniform hypertrophy and production of ground substances induced by higher stress at the inner portion of the media can explain the dynamics of the opening angle following sustained hypertension (Fig. 4b).

Changes in the active response that accompany pressure-induced remodeling were studied in [28]. Sustained hypertension was caused by legation of the aorta between the two kidneys. The results obtained showed that the capacity of the vascular SMCs to develop maximal active stress is not altered by the hypertension. The basal tone increases rapidly in the acute hypertension phase (2 to 8 days post surgery) and drops back towards control values

at 56 days after onset of hypertension. As found by other authors, the wall thickness increases over time. However, change in the vascular tone precedes the geometrical change. These findings showed that the fast change in the tone serves as a primary adaptive mechanism that tends to restore the baseline strain and stress distribution in the aortic wall in response to a change in blood pressure.

Finally, some recent *in vivo* investigations focus on the combined effects of changes in pressure and flow on arterial remodeling. Hayashi et al. [29] reported results on the response of arterial wall to the combinations of hypertension and altered blood flow. These authors showed that the arterial wall thickens to restore the baseline value of wall stress regardless of the magnitude of blood flow. Pressure-diameter relationships were recorded *in vitro* under normal conditions (Krebs-Ringer solution), under active conditions administered with norepinephrine, and under passive conditions administered with papaverine. The results obtained showed that an increase in pressure enhances the vasomotor response.

Summarizing, the *in vivo* experimental studies have shown that arteries predominately change their wall thickness in response to changes in pressure, while altered blood flow mainly affects the arterial diameter. Remodeling is directed to restore the baseline distribution of the circumferential tensile stress in the media and the baseline flow-induced shear stress at the intima.

2.2. Investigations in Organ and Cell Culture Systems

Though *in vivo* investigations keep the artery under conditions that are close to physiological, there are difficulties in controlling and monitoring precisely and continuously the mechanical environment and remodeling outputs. Moreover, other factors such as nervous stimuli and the local hormonal and metabolic environment might affect smooth muscle cell activity and wall remodeling. To focus solely on the effects of mechanical environment organ culture systems were used. They provide conditions supporting the arterial metabolism and maintaining the arterial function for a period of several days up to two weeks [30, 31]. A schematic representation of an organ culture system is shown in Fig. 5. It consists of a vessel chamber and a perfusion loop.

The advantage of the organ culture system is that it allows to keep the vessel in a well-defined chemical and nutrient environment and to eliminate the non-mechanical factors. The system allows independently to vary the

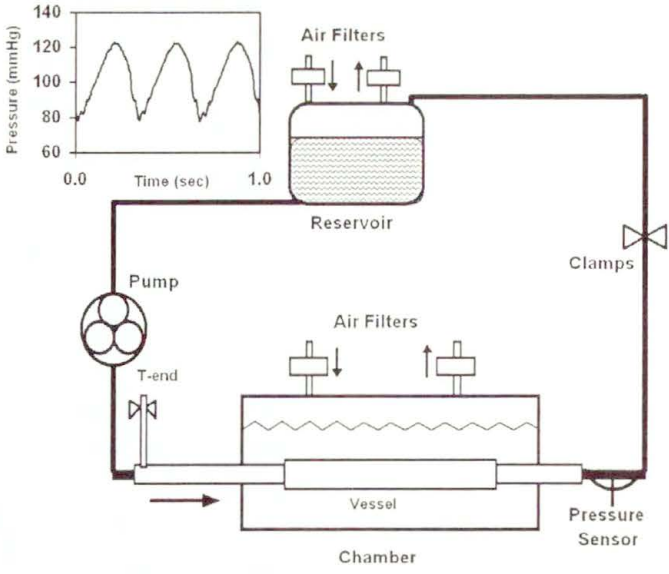

FIGURE 5. Schematic representation of an organ culture system (from [31])

magnitude and frequency of the pressure and flow, and to evaluate better their contribution to the outputs of remodeling. Because remodeling in response to altered flow takes longer than the duration in which current organ culture systems can maintain the smooth muscle cell viability, most of the investigations focus on the effects of the changes in pressure.

Mechanical and dimensional adaptation of the rabbit carotid artery in organ culture was studied by Matsumoto et al., [30]. A rabbit carotid artery was cultured for 6 days at zero mm Hg (hypotension), at 80 mm Hg (normotension) and at 160 mm Hg (hypertension). It was found that the inner diameter was not significantly different among the three groups. The wall thickness of hypertensive arteries increases, while the wall thickness of hypotensive arteries decreases compared to the normotensive vessels. The effects of increased pressure on geometrical dimensions are similar to those observed *in vivo* [22, 23]. No significant difference was found in the pressure-diameter relationship between hypertensive and normotensive groups, while arteries cultured under hypotensive conditions are less distensible.

Han and Ku studied the geometrical changes of porcine carotid arteries perfused with a physiological pulsatile flow and subject to hypertensive ($200\pm$ 30 mm Hg) and normotensive (100 ± 20 mm Hg) pressures [31]. They found that the outer diameter of the hypertensive arteries continually increases

over time, which most likely shows that the artery increases its thickness but keeps unchanged the inner diameter to maintain the baseline value of the wall shear and to adapt the medial tensile stress. These observations are again consistent with data from *in vivo* experiments. The active response evaluated from the pressure-diameter relationships recorded before and after administration of norepinephrine has shown that the hypertensive arteries manifest a stronger contractile response compared to controls.

Han et al. [32] reported data for remodeling response of arteries to axial stretch in organ culture. They found that axial mechanical stimuli increase smooth muscle cell proliferation and promote longitudinal growth.

The results from organ culture studies have shown that pressure and flow conditions are major determinants of the geometrical dimensions, mechanical properties and the active response of arteries. A limitation for use an organ culture is still the short period during which the vascular smooth muscle can be kept viable.

Investigations in organ culture provide important information for controlling the mechanical environment in bioreactors for manufacturing functional tissue engineered vascular grafts. Constructs composed of biodegradable scaffold and seeded endothelial and smooth muscle cells are subjected to changes in pressure and flow to promote neo-artery formation and to produce an arterial substitute of appropriate mechanical properties and sufficient strength.

In contrast to organ culture studies, which are performed on tubular arterial specimens, the investigations in the cell culture are addressed to study the events that occur when smooth muscle cells or endothelial cells are subjected to flow-induced shear or to constant or cyclic strains. It was found that the endothelial and smooth muscle cells change their shape, orientation, proliferation, release of vasoactive substances and matrix protein secretion [33–35]. Though a cell culture is characterized by a precise control over mechanical factors, this approach disregards the interactions among different cell types and the influence of the extracellular environment that exists under physiological *in vivo* conditions and in organ culture systems. Therefore, the results obtained from cell culture studies cannot be used to predict the geometrical and mechanical outputs of remodeling of native arteries in response to changes in their mechanical environment.

In conclusion, the experimental investigations have shown that arteries remodel their geometrical dimensions to maintain the flow-induced shear stress at the intima and the pressure-induced wall tensile stress in the media.

Remodeling of the mechanical properties is a much slower process and might aim at restoring the normal level of the arterial function. In general, remodeling represents a locally controlled adaptive response tending to cope with changes in the mechanical environment. Remodeling is preceded by a change in the smooth muscle activity that occurs as a primary adaptive response to the altered mechanical environment.

3. Mathematical Models of Remodeling

Experimental evidence shows that the arterial response to changes in pressure and flow is a local phenomenon, which can be described in terms of mechanical quantities such as strains and stresses, suggests developing mathematical models based on continuum mechanics. The results of these models aim to predict the outputs of geometrical and mechanical remodeling caused by the changes in the mechanical environment. The information is important because the dimensions and mechanical properties determine the arterial function of distributing and transporting the blood by means of a flow of moderate pulsations.

The general idea of modeling is to substitute the real object by a model, which exhibits the main characteristics of a certain class of objects under study. The results obtained as model predictions are claimed to be valid for the real object. In contrast to the experimental studies that answer *what happens*, the models aim to answer *why a certain event occurs*. Although the results of experimental studies can give insights into underling mechanisms of remodeling, these results have a limited predictive value. In fact, the vascular cells, and the smooth muscle cells in particular, sense and respond not to pressure and flow rate but to local stresses, which cannot be measured but are to be calculated using an appropriate mathematical model.

The benefit of mathematical modeling to quantify the arterial remodeling is manifold. Comparison of theoretical predictions and experimental findings justifies the acceptance or rejection of the model hypotheses introduced for mechanical quantities that drive and govern the adaptation process. If appropriate experiments do not exist, modeling can suggest the kinds of new experiments that are needed and methodology for analyzing the data. It is expected that the results obtained from continuum mechanics models may advance the level of understanding of the role that mechanical factors play during normal arterial development and maturity, and might help to reveal the mechanical aspects of the genesis and progression of certain vascular

pathologies. Additionally, results from model studies could promote the development of therapeutic interventions capable of restoring the mechanical loads on arteries to normal levels. Finally, knowledge of mechanisms underlying arterial wall remodeling can be used to design a favorable mechanical environment for tissue engineered arteries in bioreactors.

Several approaches can be applied to study theoretically soft tissue remodeling. One group of models is based on specifying balance equations for cell population accounting for their proliferation, apoptosis and migration. Such models, however, cannot include the effect of the mechanical environment using the basic categories of the continuum mechanics such as strain and stress. First attempts to study the growth in soft tissues in the context of continuum mechanics belong to Skalak [36]. The basic idea is that the growth does not result in an increase in number of the particles but as an increase in the mass of already existing particles. The author considered the result of remodeling by addressing the kinematics of the process. This idea was further developed for proposing a theory of three-dimensional *volumetric growth* [37] and was employed to study the development of arteries and their response to changes in arterial pressure and flow [38]. Models based on the volumetric growth consider an artery as a collection of growing differential elements that change their zero-stress state. Another group of models, focused on the description of the kinematics of the zero-stress configuration of the vessel as a whole, and refer rather to the *global growth* kinematics description. In this context the term growth will be used to describe changes in mass that might not be associated to the process of biological development and maturity.

Recently, Humphrey and Rajagopal [39] proposed a different approach in modeling the growth and remodeling of soft tissues by using the theory of constrained mixtures. The arterial tissue is considered as a composite material. The basic structural constituents, the elastin, collagen and vascular smooth muscle, have individual mechanical properties, individual rates of production and removal, and individual evolving natural configurations. Observed growth results from the imbalances in the production and removal of the individual constituents with rate parameters depending on the mechanical environment. This approach focuses on the processes associated with remodeling in contrast to the volumetric and global growth approach that consider the consequences of remodeling.

A brief description of volumetric growth theory, global growth approach and their use to study arterial remodeling are given in the next sections.

3.1. Volumetric Growth

Following Rodriguez et al. [37] and Taber [2] in this section we briefly present the general theory of three-dimensional volumetric growth. Consider an elastic body that at time t_0 has the stress-free configuration $B(t_0)$ (Fig. 6). After applying external loads the body instantaneously undergoes a finite deformation and takes the configuration $b(t_0)$. The kinematics of the deformation process is described by the deformation gradient tensor $\mathbf{F}_0 = \partial \mathbf{x}(t_0)/\partial \mathbf{X}$ that transforms the differential position vector $d\mathbf{X}$ in B_0 into a differential position vector $d\mathbf{x}(t_0)$ in $b(t_0)$. If the body is made of growing continuum, the deformed configuration varies over time despite the constancy of the applied load and at the moment $t = t_1$ the configuration becomes $b(t_1)$. This process can be termed as the *observed growth*. The mapping of $B(t_0)$ into $b(t_1)$ is described by the gradient tensor $\mathbf{F} = \partial \mathbf{x}(t_1)/\partial \mathbf{X}$. The deformed configuration $b(t_1)$ is a result not only of adding and/or removal of volume, i.e. the *pure growth*, but is also affected by the change in the elastic deformation. If the loads are removed at time $t = t_1$ the body takes a configuration $B''(t_1)$, which is different from $B(t_0)$ and might not be in a stress-free state but contains residual strains and stresses. Thus the no load configuration at the moment $t = t_1$ is also a result of growth and deformation.

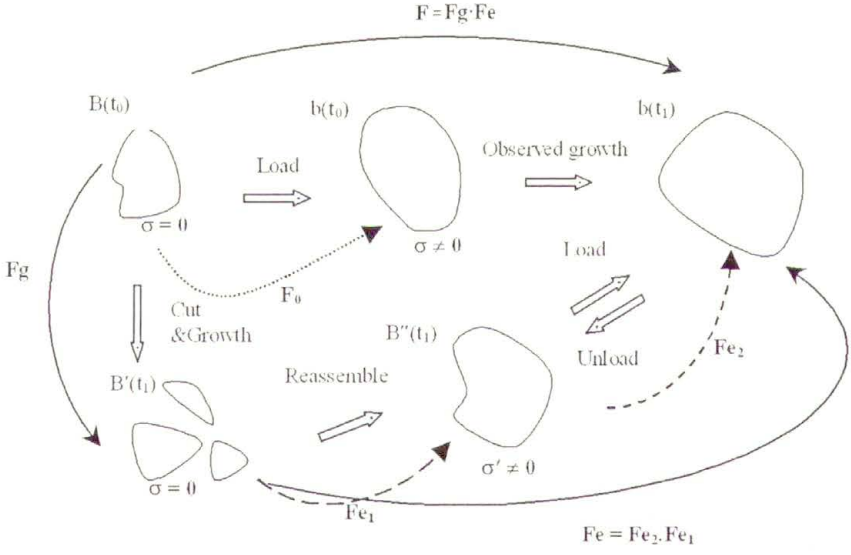

FIGURE 6. Schematic representation of configurations resulting from deformation and volumetric growth (modified from [2] and [37])

To describe the kinematics of the observed growth on the basis of the true growth and deformation process imagine that the body is divided into infinitesimal elements. Each element undergoes finite volumetric growth. This grown stress-free configuration is denoted by $B'(t_1)$ (Fig. 6) and is the result only of addition or removal of volume to or from each element. The transformation of a differential position vector is defined by the growth gradient tensor $\mathbf{F}_g = \partial \mathbf{x}_g(t_1)/\partial \mathbf{X}$, where $\mathbf{x}_g(t_1)$ is the position vector in $B'(t_1)$ of a point having a position vector $\mathbf{X}$ in $B(t_0)$. This process is not isochoric and therefore the infinitesimal volume may increase ($\det \mathbf{F}_g > 1$) or decrease ($\det \mathbf{F}_g < 1$). The grown elements in $B'(t_1)$ may not fit each other. If the growth does not destroy the continuity of the material, reassembling of elements into configuration $B''(t_1)$ requires deformation that gives rise to a stress field called the residual stresses. The mapping of $B'(t_1)$ into $B''(t_1)$ is described by the elastic deformation gradient tensor $\mathbf{F}_{e1}$. Finally, after applying the external loads, the configuration $B''(t_1)$ transforms into $b(t_1)$ and the mapping is described by the deformation gradient tensor $\mathbf{F}_{e2}$.

The total deformation that the grown body undergoes from its zero-stress state $B'(t_1)$ to the deformed state $b(t_1)$ at time $t = t_1$ is described by the total elastic deformation gradient tensor $\mathbf{F}_e = \mathbf{F}_{e2} \cdot \mathbf{F}_{e1}$. Finally, the transformation that an infinitesimal volume undergoes at an arbitrary point of the reference configuration $B(t_0)$ due to the growth and applied forces is described by the gradient tensor $\mathbf{F} = \mathbf{F}_e \cdot \mathbf{F}_g$. In this way the contribution of the pure growth is separated from the deformation that induces the stress field. To perform this decomposition it is necessary that the stress-free configuration $B'(t_1)$ is unique, which holds true for elastic materials.

Determining $\mathbf{F}_e$ and $\mathbf{F}_g$ requires solving a boundary-value problem for the coupled deformation and growth processes. Following the theory of finite deformations the corresponding Green strain tensor is $\mathbf{e} = (\mathbf{F}_e^T \mathbf{F}_e - \mathbf{I})/2$, where $\mathbf{I}$ is the identity tensor and the superscript T denotes the transpose operation. When the solid is considered to be incompressible, which is the case of most biological tissues, any deformation is isochoric and therefore, $\det \mathbf{e} = 0$.

Strains produce stresses according to the constitutive equations characterizing the mechanical properties of the solid. Because remodeling takes place on a large time scale the viscous properties cannot be taken into account. For elastic medium there exists a strain energy density function W that depends on strain tensor $\mathbf{e}$. Assuming that the mechanical properties

remain unchanged during the whole growth process and the material is homogeneous, W is a function of strain tensor $\mathbf{e}$ only. The Cauchy stress tensor $\boldsymbol{\sigma}$ defined per unit deformed area in $b(t_1)$ is

$$\boldsymbol{\sigma} = \mathbf{F}_{\mathrm{e}} \cdot \frac{\partial W}{\partial \mathbf{e}} \cdot \mathbf{F}_{\mathrm{e}}^{T} + p\mathbf{I} \tag{3.1}$$

where p is an unknown scalar function. In the absence of body forces the stress $\boldsymbol{\sigma}$ satisfies the equation of equilibrium formulated with respect to the current deformed grown configuration $b(t_1)$, $\nabla \cdot \boldsymbol{\sigma} = \mathbf{0}$, where $\nabla = \partial/\partial \mathbf{x}(t_1)$. Boundary conditions are to be described for the displacement vector defined as a difference between position vectors of the same particle in $B_0(t_0)$ and $b(t_1)$ and/or for the tractions on the bounding surface of $b(t_1)$.

Because the growth deformation gradient tensor $\mathbf{F}_{\mathrm{g}}$ is not in general known, additional information is necessary for the interrelations between $\mathbf{F}_{\mathrm{g}}$ and the tensors describing the strain and stress field in the grown body. These functional relations are called the *growth laws* and phenomenologically describe, at the continuum mechanics level, the effects of mechanical quantities on the processes of mass supply or resorption. How cells detect changes in the local mechanical environment and convert them into signals that trigger and govern the remodeling process is still unknown.

Like any objective constitutive relation, the growth laws are determined from simple experiments or identified by comparing the model predictions for typical situations with the corresponding experimental observations. In general, the growth gradient tensor $\mathbf{F}_{\mathrm{g}}$ or its rate of change may depend on the strain tensor $\mathbf{e}$, the stress tensor $\boldsymbol{\sigma}$, the strain energy density function W or on the time rates of these quantities. It seems reasonable to consider the strain as a probable candidate for a growth because changes in lengths and angles could be "sensed" by the cells. However, by definition strains are defined with respect to the zero-stress configuration that a living tissue never experiences under physiological conditions. Therefore postulating a stress-dependent growth laws was preferred. Fung proposed a mass-stress growth law of the form, [40],

$$\frac{dm}{dt} = C\,(\sigma - a)^{k_1}\,(b - \sigma)^{k_2}\,(\sigma - c)^{k_3}\,, \tag{3.2}$$

where dm/dt is the rate of mass growth, C, a, b, c, k_1, k_2, and k_3 are constants to be determined experimentally and σ is a scalar measure of current stress (e.g., mean value or stress invariant).

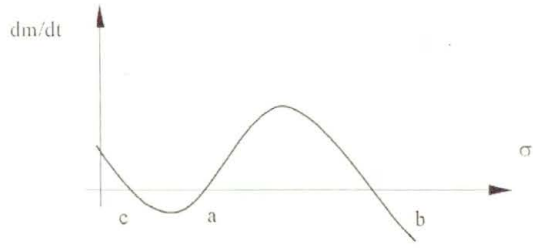

FIGURE 7. Schematic representation of growth rate-stress relation (modified from [40])

Equation (3.2), schematically illustrated in Fig. 7, shows that the stresses corresponding to the "growth equilibrium states" do not initiate a change in the mass. The deviations of stress from "equilibrium stresses" serve as driving stimuli for processes resulting in an increase or decrease of mass. Particular forms of growth laws referring to the remodeling of straight muscles, heart and arteries were proposed in [41, 42].

3.2. Model for Aortic Growth Based on Fluid Shear and Fiber Stresses

To illustrate the use of the volumetric growth approach we consider the mathematical model for growth and remodeling of a rat's aorta proposed by Taber [38]. The study addresses the hypothesis that the changes in the aortic geometry during development and in response to increased pressure are driven by the deviations of the tensile stress from its baseline value, and are modulated by the flow-induced shear stress.

Mathematical model

During the whole process of growth and remodeling the aorta was considered to be a two-layered tube made of elastic orthotropic and incompressible materials, representing the intima/media and adventitia. The vessel is inflated by an internal pressure P and is extended longitudinally. It undergoes a volumetric growth resulting in an increase in length of the elements in the radial, circumferential and axial direction. The deformed grown state $b(t_1)$ at the moment $t = t_1$ is related to the reference state $B(t_0)$ (Fig. 8) by the relations

$$r = r(R, t), \quad \theta = \Theta, \quad z = \lambda(t)Z \tag{3.3}$$

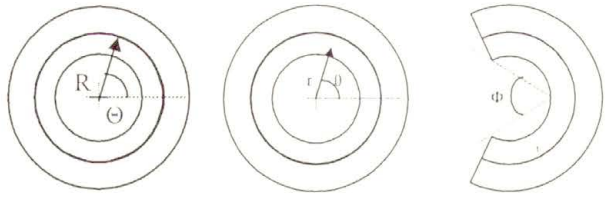

(a) (b) (c)

FIGURE 8. Schematic representation of (a) reference state $B(t_0)$; (b) deformed grown state $b(t_1)$; and (c) opened-up configuration

where λ is the axial stretch ratio[1)]. (R, Θ, Z) and (r, θ, z) are the cylindrical coordinates of a point in $B(t_0)$ and $b(t_1)$, respectively. The total stretch ratios for each layer are

$$\lambda_r = \frac{\partial r}{\partial R} = \lambda_r^* \lambda_{gr}, \quad \lambda_\theta = \frac{r}{R} = \lambda_\theta^* \lambda_{\theta g}, \quad \lambda_z = \lambda = \lambda_z^* \lambda_{zg}, \tag{3.4}$$

where λ_{gr}, $\lambda_{g\theta}$, and λ_{gz} are the growth stretch ratios with respect to the cylindrical coordinates (r, θ, z), and λ_r^*, λ_θ^*, and λ_z^* are the stretch ratios due to the deformation of the stress-free grown state into the loaded state $b(t_1)$. Due to material incompressibility the elastic deformation is isochoric and the following relation holds true $\lambda_r^* \lambda_\theta^* \lambda_z^* = 1$. The corresponding components of Green strains are $e_i = (\lambda_i^{*2} - 1)/2$, $i = (r, \theta, z)$.

Constitutive equations of the wall material relate the stresses in $b(t_1)$ to Green strains as follows

$$\sigma_i = \lambda_i^{*2} \frac{\partial W}{\partial e_i^*} + p, \tag{3.5}$$

where $W(e_r^*, e_\theta^*, e_z^*)$ is the strain energy density function; $p(r, t)$ is an unknown scalar function to be determined from the equilibrium equations and boundary conditions.

The radial equilibrium equation is

$$\frac{\partial \sigma_r}{\partial r} + \frac{\sigma_r - \sigma_\theta}{r} = 0, \tag{3.6}$$

and the boundary conditions at the inner surface, $(r = r_i)$, and outer surface, $(r = r_o)$, are

$$\sigma_r \,|_{r=r_i} = -P, \quad \sigma_r \,|_{r=r_o} = 0. \tag{3.7}$$

[1)]Strain and stress analysis of a thick-walled tube is given in Appendix A. The basic field equations are given here for completeness.

The radial stress σ_r is continuous on the contact surface between two layers. The vessel is considered to be with closed ends and the overall equilibrium in axial direction yields

$$2\int_{r_i}^{r_o} \sigma_z r dr = r_i^2 P. \tag{3.8}$$

Based on experimental observations that sustained changes in flow cause a change in radius, while persistent changes in pressure mainly affect the wall thickness, Taber postulated the following stress-based growth laws

$$\begin{aligned} \frac{\partial \lambda_{gr}}{\partial t} &= \frac{1}{T_r}\left(\frac{\sigma_\theta - \sigma_{\theta 0}}{(\sigma_{\theta 0})_m}\right), \\ \frac{\partial \lambda_{g\theta}}{\partial t} &= \frac{1}{T_\theta}\left(\frac{\sigma_\theta - \sigma_{\theta 0}}{(\sigma_{\theta 0})_m}\right) + \frac{1}{T_r}\left(\frac{\tau - \tau_0}{(\tau_0)_m}\right)\exp\left(-\alpha(R/R_1 - 1)\right), \\ \frac{\partial \lambda_{gz}}{\partial t} &= 0, \end{aligned} \tag{3.9}$$

where τ is the flow-induced shear stress on the endothelium; T_i are time constants; α is a constant characterizing the decay of the signal with distance from the inner surface; $\sigma_{\theta 0}$ and τ_0 are the growth equilibrium circumferential wall stress and flow-induced shear stress, with subscript m denoting values at maturity. It was assumed that the equilibrium stresses depend linearly on blood pressure during development, and then remain constant in the matured organism. At $t = 0$ the growth stretch ratio λ_{gr}, $\lambda_{g\theta}$, and λ_{gz} were set to be equal to one, i.e. no growth occurs.

Results and Discussion

After specifying the strain energy function and all model parameters, the governing equations were solved numerically. The results obtained showed realistic time courses of geometrical dimensions of the rat aorta during development and under hypertensive conditions (see [38]). The model predictions are in quantities agreement with the experimental data of Fung and Liu [23] and support the introduced hypothesis that mechanical forces have significant effects on the geometry of the aorta. The model suggests that the changes in aortic geometry are driven by the tensile wall stress and are modulated by the flow-induced shear stress according to the growth laws (3.9).

3.3. Global Growth Approach

The global growth approach was proposed for studying geometrical changes in arteries caused by alterations in arterial pressure [43, 44]. The basic hypothesis is that remodeling results solely in a change in the geometrical dimensions of the zero-stress configuration. The rates of change of the geometrical dimensions and the parameters that describe the strain and/or stress state of the arterial wall are related by appropriate evolution equations. Referring to the case of volumetric growth described in the previous section, this approach assumes that all changes of the differential elements are mutually compatible and no deformation is required to assemble the grown elements into a continuum body. The configurations of a growing artery are shown schematically in Fig. 9.

The mapping of the original zero-stress configuration $B(t_0)$ into a grown zero-stress configuration $B'(t_1)$ represents a homotopic transformation. The global growth approach is a particular case of the more general theory of volumetric growth and therefore has limited applicability. However, there are at least two cases when the use of this approach is justified: i) when an

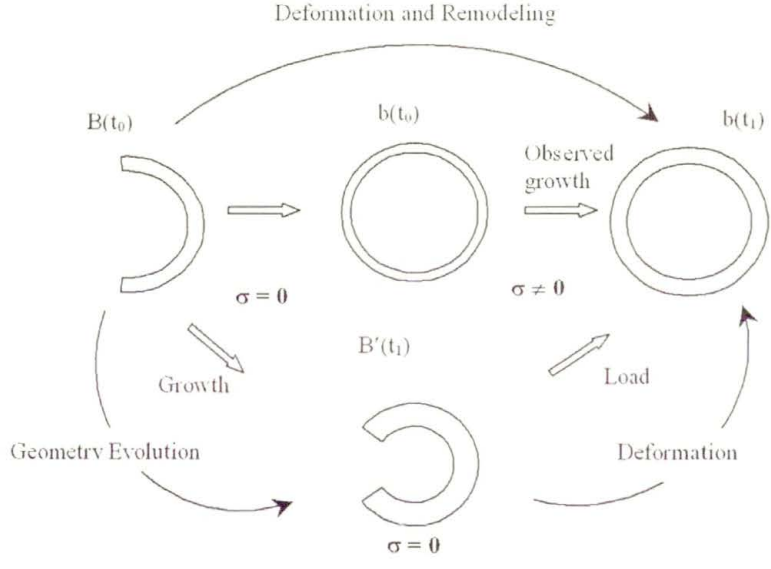

FIGURE 9. Schematic representation of the configurations resulting from deformation and global growth. $B(t_0)$ is the original zero-stress state; $b(t_0)$ is the instantaneous deformed state; $B'(t_1)$ is the grown zero-stress state; $b(t_1)$ is the grown deformed state.

artery is considered as a thick-walled tube, but it is assumed that a single radial cut releases all, or at least most of the residual stress and the opened-up configuration is stress-free; and ii) when an artery is considered to be a thin-walled elastic membrane. As shown in Appendix B in this case the state of no load is stress-free.

To illustrate the global growth approach a model of arterial adaptation to sustained changes in flow is considered in the next subsection.

3.4. Model of Arterial Adaptation to Changes in Blood Flow

Experimental investigations have shown that the arterial response to changes in blood flow involves processes in which the smooth muscle cells play a key role. Therefore, relevant modeling should include both the short- and long-term contribution of the vascular smooth muscle. A mathematical model for both the acute vasomotor response and the long-term geometrical remodeling of arteries induced by sustained changes in blood flow was proposed by Rachev [45]. The model is aimed to give a probable interpretation of some experimental results available in the literature and to suggest new types of experiments. The study addresses the hypothesis that the synthetic and proliferative activity of the smooth muscle cells, which leads to a change in arterial dimensions, is shear stress dependent and is associated with the changes in the contractile state of the smooth muscle cells. The case of remodeling in response to a persistent increase in flow is considered in this subsection.

Mathematical model

The artery is considered to be a thin membrane made of a nonlinear elastic incompressible and orthotropic material. Based on experimental findings that in some cases an artery remodels without altering significantly its structure and composition, [20, 21], the mechanical properties are considered unchanged during remodeling. Under physiological loads the artery undergoes a finite elastic deformation (see Appendix B). The stress state is calculated following the approach given in [46]. Based on Hill's functional model [1], the total circumferential wall stress per unit deformed area is

$$\sigma_{\mathrm{T}} = \sigma_{\mathrm{p}}(\lambda_\theta) + S\left(\mathrm{Ca}^{++}\right)\lambda_\theta\left(1 - \left(\frac{\lambda_m - \lambda_\theta}{\lambda_m - \lambda_0}\right)^2\right) \tag{3.10}$$

where σ_p is the passive stress that is borne by the wall material when the vascular smooth muscle cells are fully relaxed; λ_θ is the circumferential stretch

ratio. The second term in Eq. (3.10) is the active stresses developed by the SMCs when they are stimulated.

The active stress depends on the intensity of the stimulation and on the actual length at which the active stresses is generated. At a constant length and variable stimulus the active tension (the stress resultant of the active stress across the wall thickness) depends on the intensity of stimulation following the *active tension-dose relationship*. This relationship accounts for the level of the contractile activity of SMCs, which in turn depends on the intercellular concentration of the free calcium ions (Ca^{++}). It has been established that in the homeostatic state the relationship between the developed active tension and the free calcium concentration is close to a sigmoid function, exhibiting a pronounced linear portion over the physiological range of stresses [47]. On the other hand, the magnitude of the active tension developed at constant arterial diameter (under isomeric contraction) and constant stimulus depends on the actual diameter following the *active tension-diameter* relationship [48]. It was found that this relationship is close to parabolic function. There exists an optimal deformed diameter at which the active tension developed by the SMCs has a maximum value, while below and above certain values the active tension is zero. The parameter S in Eq. (3.10) represents the maximum active stress per unit undeformed area (*Lagrangian stress*) for given intensity of stimulation and at stretch ratio λ_m corresponding to the optimal deformed diameter. S is a measure of the muscular activation and depends on the ionic state of the VSMs. Therefore the parameter S characterizes the intrinsic capability of developing an active stress by the vascular muscle at given stimulation. The value of the feasible active stress depends on active tension-diameter relationship; λ_0 is the stretch ratio at which the activation is ceases. The factor λ_θ accounts for the fact that the actual active stress (*Cauchy stress*), is defined per unit deformed area.

The equation of overall equilibrium of the vessel in the radial direction (see Appendix B, Eq. (B.6)) reads

$$\sigma_{\theta p}(\lambda_\theta) + S\lambda_\theta \left(1 - \left(\frac{\lambda_m - \lambda_\theta}{\lambda_m - \lambda_0}\right)^2\right) - P\left[\frac{\lambda_z \lambda_\theta^2 R}{H} - \frac{1}{2}\right] = 0 \qquad (3.11)$$

where P is the applied arterial pressure and λ_z is the axial stretch ratio. R and H are the mid-wall radius and wall thickness at the state of no load and no muscular tone ($S = 0$).

Evolution equation for the contractile state of vascular smooth muscle

The artery is first considered under conditions at which the pressure, flow and muscular tone (activation parameter S) have their baseline values P_0, Q_0, and S_0, respectively. The mid-wall radius and the wall thickness in the unloaded state are denoted by R_0 and H_0. Hereafter, the subscript "zero" will be used to refer to the artery under normal flow conditions. The mean flow rate is changed in a step-wise manner from Q_0 to Q^* and kept constant, while the pressure remains constant at its baseline value. At the moment of the flow jump, the vessel maintains its inner radius at the control value r_{i0}. According to Eq. (2.1) the change in the flow rate causes an instantaneous jump in the shear stress at the arterial lumen from τ_0 to $\tau' = \tau_0(Q^*/Q_0)$. Over time the magnitude of the shear stress varies via the changes in the inner radius caused by the vasomotor response and geometrical remodeling.

Exploiting the experimental observations that for mature vessels the amount of major structural components of the wall material remains unchanged [20, 21], it is assumed that the ratio of the area occupied by the smooth muscle cells and the total area remains constant during the whole process of remodeling. Therefore, the parameter S depends only on the intensity of stimulation via the changes in the calcium concentration within the cells. The functional relationship between S and the concentration of Ca^{++} is assumed linear over the interval of physiological interest.

The equation that describes the dynamics of S is deduced from the processes that control the calcium concentration. The basic mechanisms which lead to an increase of Ca^{++} concentration are: i) the incoming flux of calcium ions due to a concentration drop between the cell and its environment; and ii) the release of Ca^{++} from intercellular stores such as the sarcoplasmatic reticulum, where the ions are in the weakly bound form. On the other hand, there exist simultaneous processes, which cause a decrease in Ca^{++} concentration. These processes are: i) the active transport outside of the cell by the calcium pumps, ii) the sodium-calcium exchange mechanisms, and iii) the resorption of Ca^{++} in the sarcoplasmatic reticulum. Following the phenomenological approach proposed in [49] and its modification given in [50], the rate of change of calcium concentration in the smooth muscle cells, c, is described by the following balance equation

$$\frac{dc}{dt} = \varphi - \frac{1}{T}c. \tag{3.12}$$

The non-negative function φ accounts for the processes that lead to an in-

crease in the calcium concentration. The value of φ depends on the applied stimulus taking into account the coupling between the stimulus and the transmembrane flux through receptor-operated channels or release of calcium from intracellular stores. The second term on the right hand side of Eq. (3.12) takes into account the decrease of calcium within cells, which is assumed to be proportional to the actual Ca^{++} concentration. T is a positive constant that gives the decay rate of the calcium concentration.

It was assumed that the deviation of φ from its baseline value is proportional to the deviation of the shear stress, i.e. $\varphi - \varphi_0 = -\beta(\tau - \tau_0)$, where β is a positive coefficient of proportionality. This relation phenomenologically accounts for the effects of the altered shear stress at the endothelium on the membrane permeability and release of calcium from internal sources. In keeping with the experimental observations an increase in shear stress over its baseline value causes a decrease in φ leading to a decrease in intercellular Ca^{++} concentration. This initiates relaxation of the vascular smooth muscle. A decrease in shear stress under its baseline value has an opposite effect on Ca^{++} concentration and leads to contraction of the smooth muscle cells.

Using the linear dependence of the active tension on Ca^{++} concentration, [47], and introducing a dimensionless variable, the equation for the evolution of the muscle activation takes the following form

$$\frac{d\tilde{S}}{dt} = \frac{1}{T_{S1}}\left(1 - \frac{\tau}{\tau_0}\right) + \frac{1}{T_{S2}}\left(\tilde{S} - 1\right), \tag{3.13}$$

where $\tilde{S} = S/S_o$. T_{S1} and T_{S2} are time constants.

Remodeling rate equations for the case of increased flow

Following the global growth approach, the dynamics of wall remodeling is described by evolution equations for the mid-wall radius and wall thickness in the unloaded state. Generalizing the experimental observations for growth and remodeling of tissues, Rodbard [51], has proposed that tension applied to a relaxed muscle causes its longitudinal growth. Allowing for this hypothesis, the compensatory enlargement in response to an increased flow is assumed to be driven by the increased passive circumferential stress. Moreover, an increase in the total circumferential stress elicits transversal remodeling, which provides sufficient wall thickness to restore the normal value of the total circumferential stress as shown in [22, 23]. Introducing the dimensionless variables the remodeling rate equations that are in agreement with this

remodeling scenario are

$$\frac{d\tilde{R}}{dt} = \frac{1}{T_R}\left(\frac{\sigma_p}{\sigma_{p0}} - 1\right), \quad \frac{d\tilde{H}}{dt} = \frac{1}{T_{H1}}\left(\frac{\sigma_T}{\sigma_{T0}} - 1\right), \tag{3.14}$$

where $\tilde{R} = R/R_0$ and $\tilde{H} = H/H_0$; T_R and T_{H1} are time constants; and σ_T is the total circumferential stress.

The evolution equation (3.13) and the remodeling rate equations (3.14) represent a system of non-linear autonomous equations. They are coupled to the equations that describe the deformation and the equilibrium of the artery (see Appendix B), and the equation for the flow-induced wall shear stress, Eq. (2.1). The initial conditions at the onset of the step change in flow are

$$\tilde{S}(t_0) = 1, \quad \tilde{R}(t_0) = 1, \quad \tilde{H}(t_0) = 1. \tag{3.15}$$

Results and Discussion

The model parameters were identified from the experimental data for a canine carotid artery and the governing equations were solved numerically [45].

Figure 10 illustrates the time course of the dimensionless initial mid-wall radius, thickness, deformed inner radius, and the muscle tone. The non-monotonic pattern of variation of $\tilde{S}$ (Fig. 10(d)) and stretch ratio λ_θ (not shown), as well as the constancy of the undeformed arterial thickness and mid-wall radius during the early period of flow alteration (Figs. 10a–b) show that the vessel response is initially due to arterial dilatation. As geometrical remodeling proceeds, however, the initial dimensions increase slowly and monotonically to their adapted values. Simultaneously, the muscle cells restore their normal ionic state ($\tilde{S} = 1$) and the circumferential stretch ratio returns to its baseline level. Hence, the vessel restores both the passive and active stress, as they exist under normal flow conditions.

Shear deformation of the endothelial cells appears to be the first in the chain of events that result in smooth muscle relaxation or contraction. The ability of the endothelial cells to sense the deviations of the shear stress from its normal level might be impaired due to endothelial dysfunction or decreased deformability of the cells. Theoretical predictions of the model for the case of large values of the time constant T_{S1}, simulating very slow or even missing sensitivity to flow-induced shear stress, show that the ionic state in the smooth muscle cells remains practically unchanged (lines 4 in Fig. 10). Therefore, neither fast vasomotor adjustment of the arterial radius nor geometrical remodeling occurs. The conclusion that remodeling is endothelium

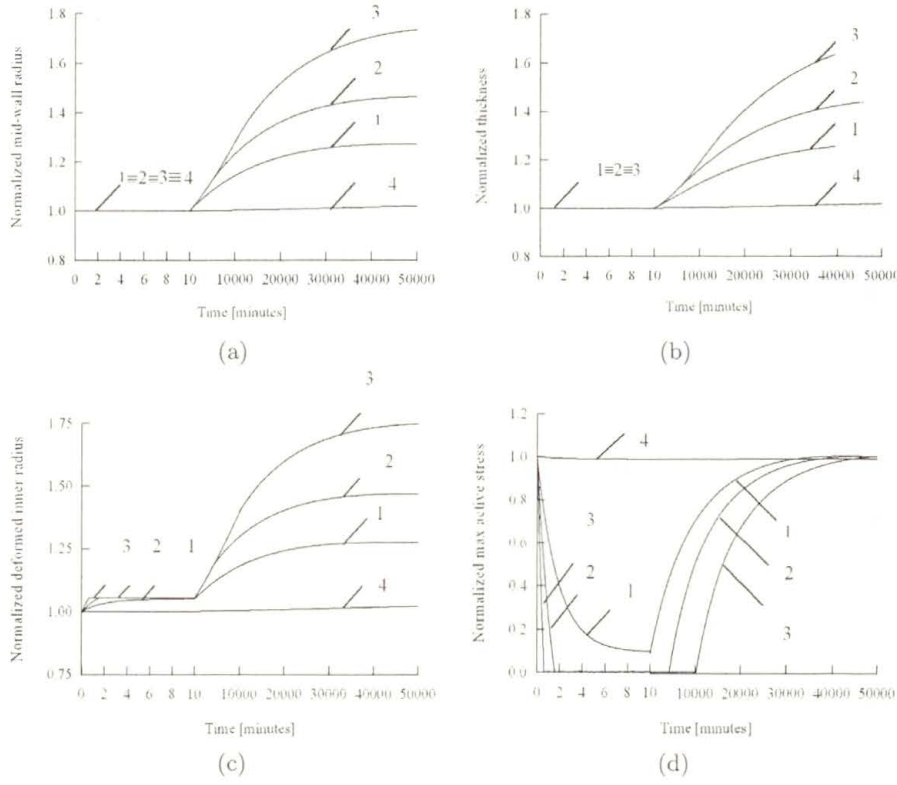

FIGURE 10. Time course of (a) normalized initial mid-wall radius $\tilde{R} = R/R_0$; (b) normalized initial wall thickness $\tilde{H} = H/H_0$; (c) normalized deformed inner radius $\tilde{r}_i = r_i, r_{i0}$; (d) normalized tone (normalized maximal active stress) $\tilde{S} = S/S_0$ after increasing blood flow by factors of two (line 1), three (line 2) and five (line 3). Line 4 refers to the case of a twofold increase in flow and a tenfold increase in the time constant T_{s1}.

dependent is in agreement with experimental observations for lack of a flow-induced response in arteries denuded of endothelium.

So far, a deviation of flow-induced shear stress from its baseline value has been recognized to be the single mechanical parameter that serves as a mediator between changes in blood flow and geometrical remodeling. The abrupt change in the shear stress, however, could be completely diminished, as a result of a vasomotor adjustment of the arterial lumen to altered flow conditions. It seems reasonable to seek interrelations between the rate of change of arterial dimensions and other mechanical values that originate from the changes in flow and persistently remain altered while the artery remodels. The basic hypothesis in this study is that geometrical remodeling

is associated with the sustained changes in the contractile state of the smooth muscle cells, which are modulated by the flow-induced shear stress sensed by the endothelial cells. The altered contractile activity affects the stress and strains experienced by the smooth muscle cells and thereby might enhance their secretory function, as well as the pattern and the rate of cells growth and division.

The model describes both the acute vasomotor response and the chronic geometrical remodeling that follow a change in blood flow. The theoretical predictions that remodeling is a stable process and results in restoration of the baseline values of the wall shear stress under normal conditions are in agreement with experimental observations available in the literature [10–12]. The results obtained also show that the ionic state of the vascular smooth muscle cells reverts to the normal homeostatic state and the muscle restores its contractile activity to the control level, which is in keeping with the findings of Hayashi (2000, private communication).

In summary, this study proposes a relatively simple mathematical model in terms of continuum mechanics. The model does not implicitly account for the series of interrelated electrical, chemical, mechanical and biological processes involved in the smooth muscle contraction and relaxation, regulation of vascular cell mitosis and apoptosis rates, cell migration, control of matrix synthesis and degradation, and regulation of matrix reorganization. The study focuses on three main events that occur after a change in blood flow: i) a change in the ionic state of smooth muscle cells caused by the altered shear stress sensed by the endothelium; ii) a change in the stress state in the arterial wall due to the altered muscular tone; and iii) a change in the geometrical dimensions of the arterial cross-section due to remodeling. The model suggests a plausible hypothesis and predicts the main features of the arterial response to a sustained increase in blood flow.

The thin-wall membrane model used in this study disregards the differential growth across the wall and the contribution of residual strains. Further generalizations of the model should consider arteries as thick-walled tubes and the effects of residual stress should be taken into account. Modified equations for evolution of muscular tone and geometrical dimensions and mechanical properties are needed for modeling flow-induced remodeling of arteries during development and maturation. In these cases the fractions of the basic structural components of the arterial wall vary over time, which affects the magnitude of the active stress. Finally, there exists a persistent

need of more experimental data, which can be used for specifying the model parameters and verifying the theoretical predictions.

4. Specific Biomechanical Problems Associated with Arterial Remodeling

Vascular diseases are leading cause of death in Western countries. As it was mentioned in the introduction, narrowing or blockage of an artery, called the *stenosis*, caused by atherosclerosis, might lead to insufficient blood supply to the tissues distal to the diseased artery. Reduced flow disturbs the normal function of the organ and may lead to a gradual or sudden death of the tissue. When a stenosis occurs in the arteries that supply blood to the brain it may lead to a stroke, while when a stenosis occurs in the coronary arteries that supply the heart muscle, it may lead to a heart attack. Substitution or bypassing of a stenosed part of an artery by a vascular graft, or performing a balloon angioplasty followed by a stent deployment is a common procedure in the vascular surgery. A stent is a wire mesh tube inserted into stenosed portion of an artery to hold it open and thereby to restore the normal blood flow.

Unfortunately, in many cases the treatment of the stenosed arteries is followed by an undesirable occlusive response called the *restenosis*. Restenosis is a result of neointima formation, termed the intimal hyperplasia, and also partly a result of proliferation of the vascular smooth muscle cells in the media. Because graft or stent deployment affects the mechanical environment of the treated artery, it is reasonable to consider restenosis as an outcome of a remodeling response. Understanding the origin of this process and the factors on which it might depend could promote better design and selection of arterial grafts and stents and may suggest improvements in surgical techniques to minimize undesirable remodeling.

Unsatisfactory results in using small caliber synthetic grafts motivate investigations for alternative vascular substitutes. Tissue engineering, based on fabricating a construct that comprises of living cells and synthetic scaffold, provides a promising solution for replacement diseased arteries. One strategy is to fabricate a resorbable graft having sufficient strength and appropriate properties to be directly implanted and to attract cells to migrate to it. During scaffold resorption a newly developed arterial tissue progressively organizes to form a functional substitute that resembles a native artery. Another approach is based on growing cells on a bioresorbable or durable scaffold *ex*

vivo in a bioreactor and subjecting the construct to appropriate chemical and mechanical stimulation until the newly developed arterial substitute is suitable for implantation. Adopting the paradigm that tissue engineering of an arterial graft should mimic the processes of natural development, growth, and maturation, modeling in terms of continuum mechanics can be beneficial for design and fabrication of novel functional arterial prostheses.

Two problems addressed to improvement the patency rate of the existing grafts by controlling the factors that promote undesirable remodeling are considered in this section. After, a simple mathematical model for regeneration of a neo-artery over a resorbable graft is considered.

4.1. New Principle to Control the Flow-Induced Remodeling in an Arterial Segment

Restenosis due to intimal hyperplasia occurs at a high rate after balloon angioplasty followed by a stent deployment and is the major negative outcome that compromises the therapeutic intervention. There exists a great deal of evidence that intimal hyperplasia is initiated and modulated by the reduction of the wall shear stress. It seems reasonable to accept that arterial restenosis is a compensatory response tending to restore the baseline value of the wall shear stress when the blood flow is reduced [18]. A strategy for preventing restenosis could be an appropriate increase in the local wall shear stress within a portion of an artery where restenosis may occur. Because it is not possible to keep locally an increased blood flow, an alternative approach to affect the shear stress is to alter the velocity profile inside the arterial region. An original idea in that respect has been proposed by Stergiopulos [52]. The keystone is to insert a small cylindrical body in the streaming line of the flow that disturbs the velocity but does not significantly affect the local flow and the hemodynamic resistance. This principle is illustrated in Fig. 11. An insert with diameter one-third of the arterial lumen causes a two-fold increase in the

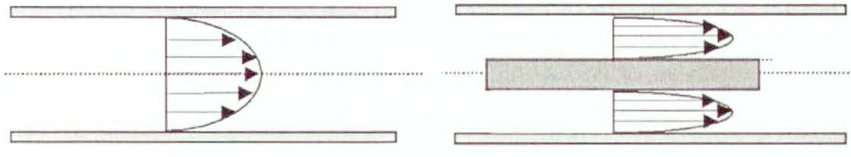

FIGURE 11. Schematic representation of velocity profiles in absence and in presence of a cylindrical insert (from [52])

wall shear accompanied by a negligible augmentation of the total resistance. Recent animal experiments with an ARES stent designed and manufactured on this principle confirmed its suitability and usefulness in preventing arterial restenosis.

4.2. Stress-Induced Geometrical Remodeling of Vessel Segments Adjacent to Stents and Artery/Graft Anastomoses

Experimental studies have shown that in the zone adjacent to an implanted Palmaz-Schatz stent the arterial lumen decreases due to wall remodeling. The wall thickening gradually decreases with distance from the stent edges [53]. Marked thickening also occurs at the artery/graft anastomoses, especially when low compliance synthetic grafts were used [54, 55]. On the other hand, theoretical studies revealed that marked increase in the axial and circumferential stresses appears in the zones close to an end-to-end anastomosis of a graft and a host artery [56–58].

It was shown in the previous sections that arteries change their geometry in response to alterations in their mechanical environment tending to restore the baseline values of the flow-induced shear stress and pressure-induced wall tensile stress. It is reasonable to expect that the observed change in the arterial thickness close to a stent or graft represents an adaptive response to the stress concentration. However, if remodeling is considered to be driven exclusively by the wall stresses, there is no a priori reason to expect that this process is self-limiting. A theoretical study addressed to this issue was performed in [59].

Mathematical model of the arterial wall

An artery was considered as a long cylindrical shell of constant midwall radius and constant wall thickness. The shell is considered clamped at the junction to a graft or stented arterial region. Justification of this assumption is the fact that the currently approved clinical grafts and stents are much stiffer than the native arteries. The arterial material is assumed to be elastic, incompressible and orthotropic with axes of orthotropy in the axial and circumferential direction. The artery is extended longitudinally to its in situ length and is subjected to a variable internal pressure. Given the load, initial dimensions, and prescribed boundary conditions, the wall stresses can be calculated. It is hypothesized that when the magnitude of the stresses

exceeds certain threshold values the wall thickens according to a postulated remodeling rate equation and the vessel becomes a shell of variable thickness.

To calculate the stresses that exist in the arterial wall at an arbitrary moment, the deformation process is divided into two stages. First, the artery is considered apart from the graft or stented region as a cylindrical membrane of constant mid-wall radius and of variable wall thickness. The membrane is extended to its in situ length and is inflated by the mean arterial pressure undergoing a finite axisymmetric deformation. The membrane stresses σ_m and their resultants N_m are calculated as given in Appendix B, (Fig. 12). The subscripts 1 and 2 refer to the axial and the circumferential direction, respectively and x_1 is the axial coordinate measured from the clamped cross-section along the deformed membrane.

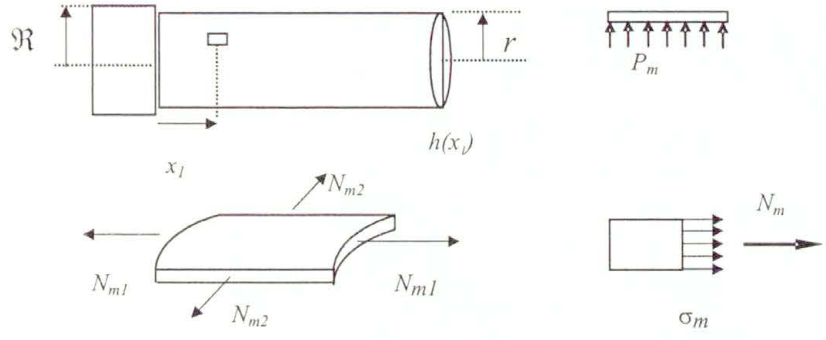

FIGURE 12. Schematic representation of the membrane state

The real artery is clamped at the anastomosis and is subjected to pressure that varies from the diastolic to systolic value. Therefore, after being finitely extended the artery is subjected to an additional axisymmetric deformation caused by clamping and by additional variable pressure. In this stage, the vessel is considered to be a long prestressed cylindrical shell subject to inflation and bending. The middle surface undergoes an additional displacement with component $w(x_1)$ in the radial direction, which is considered small compared to the wall thickness. The displacement in the axial direction was assumed to be zero in agreement with the experimental observations for the tethering effect of the tissues surrounding the artery during pressure variation. The stress resultants due to this deformation are the axial and circumferential tensile tensions, the axial transverse force and the axial and circumferential bending moments. They are denoted by prime and are shown in Fig. 13.

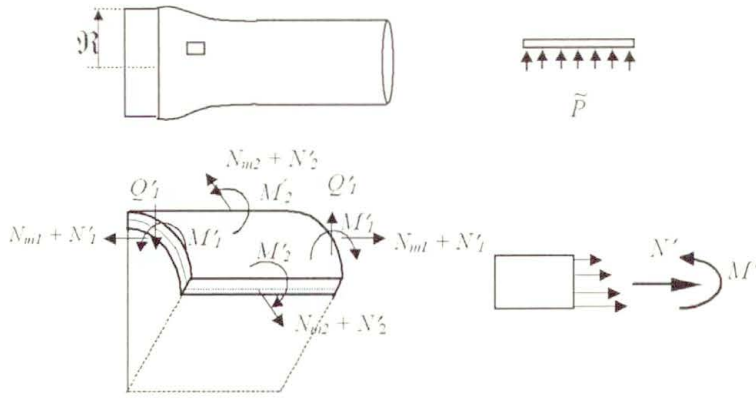

FIGURE 13. Schematic representation of the bending state

Following the linear theory of cylindrical shells, the radial displacement w satisfies the following differential equation

$$\frac{d^2}{dx_1^2}\left[D(x_1)\frac{d^2}{dx_1^2}w\right] + G(x_1)w - N_{m1}\frac{d^2w}{dx_1^2} = \tilde{P}, \tag{4.1}$$

where

$$D(x_1) = \frac{E_1 h^3(x_1)}{12(1-\mu_1\mu_2)}, \quad G(x_1) = \frac{E_2 h(x_1)}{(1-\mu_1\mu_2)r^{*2}}. \tag{4.2}$$

$h(x_1)$ is the wall thickness; r^* is the mid-wall radius in the membrane deformed state; E_1, E_2, μ_1 and μ_2 are the incremental elastic moduli and coefficients of transversal deformation, which characterize the linearized mechanical behavior of the shell around its membrane deformed state. Making use of the theory of small deformations superposed on finite deformation for the case of cylindrical shells they are calculated in [59]; $\tilde{P}$ is the variable pressure, which changes from $P_d - P_m$ to $P_s - P_m$ during the cardiac cycle. P_s and P_d are the systolic and diastolic pressure and P_m is the mean arterial pressure.

The boundary conditions at the clamped cross-section $x_1 = 0$, are

$$w = \mathfrak{R} - r^*, \quad \frac{dw}{dx_1} = 0, \tag{4.3}$$

where $\mathfrak{R}$ is the graft or stent radius at the anastomosis.

The stresses due to bending are linearly distributed across the wall thickness and have their extreme values at the inner at the outer wall surface.

The total stress is sum of the stress due to the finite membrane deformation and the stress due to the additional bending deformation. Far away from the anastomosis the artery does not experience bending and the stress field corresponds to the membrane deformed state.

Remodeling rate equation

Equation (4.1) contains two unknown functions, $w(x_1)$ and $h(x_1)$. Another differential equation for $w(x_1)$ and $h(x_1)$ is derived assuming a stress-induced wall thickening of the artery. It is postulated that the thickness changes at a rate that is proportional to the weighted sum of the deviation of the current circumferential and axial total stresses from the values existing far away from the clamped edge and calculated for the systolic pressure

$$\frac{\partial h(x_1,t)}{\partial t} = \frac{h^*}{T}\left[\alpha\left(\frac{\langle\sigma_1(x_1,t)\rangle - k\sigma_1^s}{\sigma_1^s}\right) + (1-\alpha)\left(\frac{\langle\sigma_2(x_1,t)\rangle - k\sigma_2^s}{\sigma_2^s}\right)\right]. \tag{4.4}$$

$\langle\sigma_1(x_1,t)\rangle$ and $\langle\sigma_2(x_1,t)\rangle$ are the axial and the circumferential stress, averaged across the thickness and over one heart cycle, [59]; σ_1^s and σ_2^s are the membrane stresses corresponding to systolic pressure, $\alpha \leqslant 1$ is a weighting coefficient, which accounts for the different contribution of the axial an circumferential stress to remodeling process; $k \geqslant 1$ is a coefficient that specifies the threshold values of the stress increments that initiate remodeling; T is a time constant; and h^* is the membrane thickness far from the clamped cross-section.

Results and Discussion

To obtain theoretical results from the proposed mathematical model, the model parameters were specified for a canine carotid artery and the governing equations were solved numerically using the finite difference method and an explicit time step [59].

The predicted time course of the wall thickness at the clamped region ($x_1 = 0$) from the onset of stent/graft implantation is shown in Fig. 14 for different values of the parameter k. A similar monotonic behavior in the time variation of thickness was noted at other locations.

Figure 15 illustrates the predicted variation of the wall thickness in the final adapted state for different values of the parameter k. It is seen that thickening is localized in the regions close to the anastomosis. The thick-

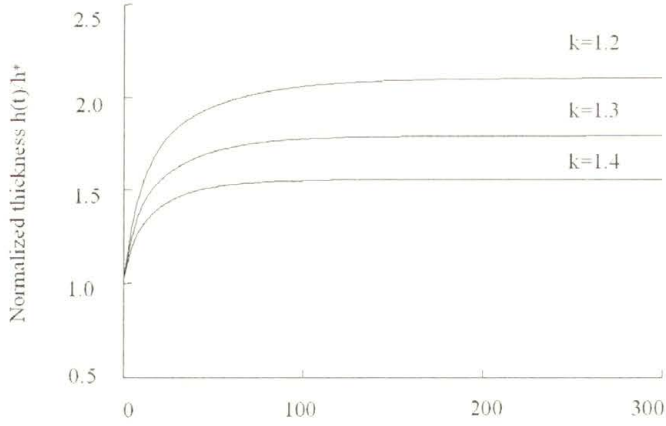

FIGURE 14. Predicted time course of the normalized wall thickness at the clamped region ($x_1 = 0$) from the onset of stent/graft implantation for different values of the parameter k

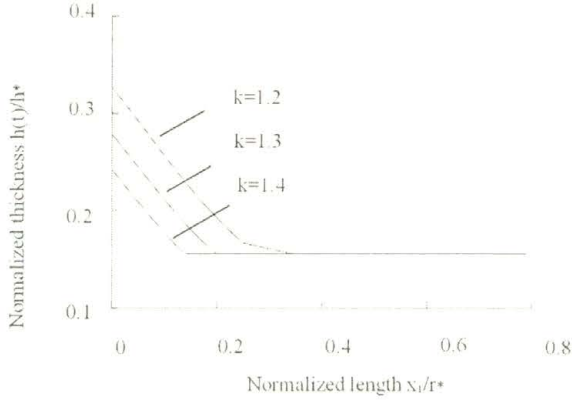

FIGURE 15. Predicted variation of the normalized wall thickness in the final adapted state for different values of the parameter k

ness gradually decreases with the distance form the anastomosis and asymptotically attains its "normal" value. These results agree with the reported experimental findings [53–55].

The axial stress variation along the vessel in the final adapted state compared to the stresses existing at the onset of graft or stent deployment is given in Fig. 16. As expected, wall thickening reduces the stress concentration in zones adjacent to the clamped cross-section. Therefore, if the stress concentration is accepted as a major determinant of vessel wall remodeling, the

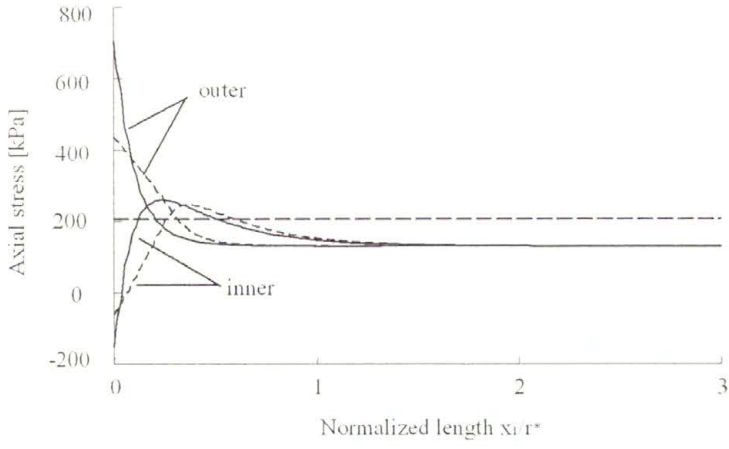

FIGURE 16. Predicted variation of the axial stress at the inner surface and outer surface at diastolic pressure $P_S = 60\,\text{mm Hg}$; $k = 1.2$. Solid lines refer to the moment immediately after stent or graft implantation; dashed lines—for the final adapted state. The horizontal line corresponds to the stress existing before implantation of a stent or a graft for systolic pressure $P_S = 140\,\text{mm Hg}$.

model predicts that the process is self-limiting and leads to local thickening of the host artery in the vicinity of an implanted stent or graft.

Despite of predicted stability in the remodeling process, in the case of pronounced increase in wall thickness some assumptions on which the model is based might not remain valid and need improvement. Consideration of an artery as a thin shell requires the deformed wall thickness to be significantly less than the mid-wall radius. In the general case, the strain and stress analysis have to be performed using appropriately developed FEM for finite nonlinear elastic deformations.

The model assumed that the increase in thickness was symmetric about the mid-wall surface, but this may not be the case in vivo. Determining of the real distribution of the new material across the arterial cross-section requires more detailed experimental investigations than have previously been performed. Mechanical properties and muscular tone were considered unchanged during remodeling and the arterial wall was considered as one-layered shell made of homogeneous material. Experimentally observed by some authors, [60], hypercompliant zones near vascular anastomosis might results from local stress induced changes in the wall material. A theoretical test of such a hypothesis requires consideration of an artery of variable mechanical properties in the axial direction.

Finally, if a stress-induced wall thickening is very pronounced, the effects of an altered flow patterns near junction might play a significant role in arterial remodeling and cannot be disregarded. In fact, stent and graft failure, including restenosis and lumen obliteration, are likely due to the combined effects of the abnormal flow-induced shear stresses at the intima and the tensile stresses in the media. This study was aimed, however, not to simulate conditions and consequences which lead to stent or graft failure, but rather to find the range of model parameters for which abnormal wall thickening occurs within admissible limits. However, the appropriate choice and motivation of the remodeling rate equation remain a key issue for further investigations.

4.3. Model of Arterial Regeneration over Bioresorbable Grafts

4.3.1. Introduction. There is a pressing need to improve the patency rate of small caliber synthetic grafts because of their unsatisfactory clinical results. This motivates an increasing interest in use of bioresorbable materials for fabricating vascular prostheses. They are made of absorbable lactide/glicolide copolymers. During post-implant time the graft dissolves due to hydrolysis and enzymatic degradation and forms a temporary scaffold for tissue ingrowth. In the early implanted phase, which lasts from one to two weeks, the graft resorbs, becoming thinner and softer. Simultaneously a thin and soft inner layer and outer layer develop. Over time these layers, and predominantly the inner one, thicken and the material gradually increases its stiffness. The rate of ingrowth parallels the kinetics of the resorption of the graft. After approximately two to three months the graft is practically resorbed. The growth and strengthening of the arterial tissue continue in a phase of maturation until the process of formation of a neo-arterial conduit is complete. Figure 17 shows the experimentally recorded time course of the thickness of the inner neo-artery layer when the resorbable graft is made of different synthetic materials.

The interrelation between the resorption process and the factors driving the arterial regeneration are poorly understood. It seems that, there exists only one theoretical investigation devoted to the analysis of the stress distribution in the resorbable graft/neo-artery complex [62]. The authors used the classical Lamé solution for a three-layered tube to study the effects of thickness and modulus of the graft and neo-artery on the stress distribution in each layer. It was found that in the early resorption phase the neo-artery is

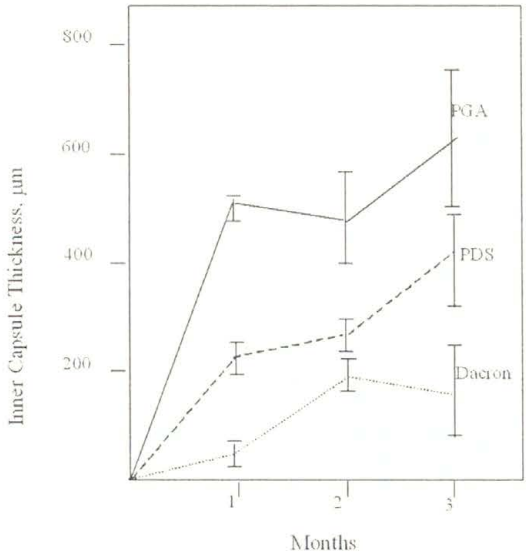

FIGURE 17. Time course of the inner layer thickness for different graft materials (from [61])

subjected to compressive circumferential stresses, suggesting the hypothesis that the compressive stresses promote the neo-artery formation. No coupling between the dynamics of the neo-artery formation and the strain and stress state in the vessel wall was considered.

During development of a neo-artery the arterial pressure and blood flow remain practically unchanged. However, any decrease in graft thickness or softening of graft material causes a redistribution of the load in the artery/graft complex. Therefore, the stresses and strains experienced by the neo-arterial tissue vary in time. It is reasonable to assume that the mechanisms leading to formation of a neo-artery are, at least in part, similar to mechanisms of arterial remodeling in response to mechanical factors. A theoretical model to test this hypothesis and to estimate the effects of certain mechanical and geometrical parameters of the graft on neo-artery formation was proposed in [63, 64].

4.3.2. Mathematical model. The neo-artery/graft complex is considered to be a thick-walled tube. At the moment immediately after graft implantation it consists of one layer representing the bioresorbable graft (Fig. 18a). During graft resorption and neo-artery formation the tube is comprised of

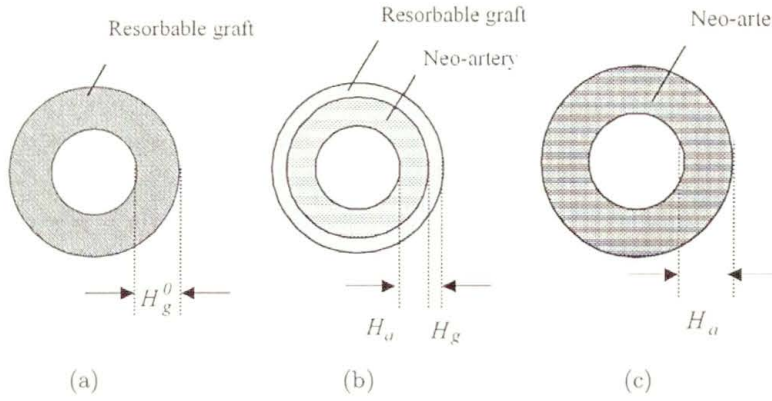

FIGURE 18. Schematic representation of the cross-sections of (a) the graft immediately after implantation; (b) the neo-artery/graft complex; and (c) the neo-artery during maturation

two layers (Fig. 18b). Justification of this simplifying assumption is the conclusion drawn in [62] that the outer neo-arterial layer does not have significant contribution to the load bearing. Finally, after the graft is completely resorbed but the neo-artery formation is still in progress, the tube is considered again as a single layered (Fig. 18c). Both the artery and graft material are assumed to be elastic, incompressible and orthotropic. Under applied loads the tube undergoes an axisymmetric finite deformation and is in the state of plane strain. The arterial pressure and blood flow rate are considered to be constant during the entire process of neo-artery formation.

The stress and strain analysis of the neo-artery/graft complex follows the method described in Appendix A. The strain energy density functions for the material of the neo-artery and the graft are chosen to be quadratic functions of the Green strains [65, 66]

$$W_k = A_k e_\theta^2 + B_k e_\theta e_z + C_k e_z^2, \quad k = a, g \tag{4.5}$$

where A_k, B_k and C_k are material constants. The subscripts a and g refer to the artery and graft, respectively.

The resorption of the graft is accompanied by softening of the material, while the regenerated neo-arterial tissue increases its material stiffness. Due to lack of experimental data for the manner in which the material constants A, B and C vary during the process of neo-artery formation and graft resorption, it is accepted that at any moment the constants B and C change proportionally to the constant A.

The constant A_g of the graft material is assumed to decrease in a linear manner during post-implant time

$$A_g(t) = A_g^0(1 - \alpha t), \tag{4.6}$$

where A_g^0 is the value at the moment of graft implantation, and α is a constant characterizing decay rate.

Consistent with some experimental observations the inner radius of the neo-artery/graft complex is considered constant over time. In keeping with the remodeling response of a healthy artery to sustained changes in pressure, thickening of the neo-artery is assumed to be driven by the deviation of the current circumferential stress borne by the vascular tissue from some "equilibrium" physiological stresses. The neo-artery regenerates by growing outwards according to the following remodeling rate equation

$$\frac{dH_a(t)}{dt} = \begin{cases} \frac{1}{T_1}\left(\frac{\sigma_a - \sigma_\theta}{\sigma_b}\right) & \text{if } \sigma_\theta < \sigma_a, \\ 0 & \text{if } \sigma_a < \sigma_\theta < \sigma_b, \\ \frac{1}{T_2}\left(\frac{\sigma_\theta - \sigma_b}{\sigma_b}\right) & \text{if } \sigma_\theta > \sigma_b \end{cases} \tag{4.7}$$

where $H_a(t)$ is the current undeformed thickness; σ_θ is the current mean circumferential arterial stress; σ_a and σ_b are the "equilibrium" physiological stresses; and T_1 and T_2 are constants that depend on rate at which the neo-arterial tissue develops. Equation (4.7) states that the rate of change of H_a depends linearly on the deviation of the current mean arterial stress from certain values, which do not elicit arterial remodeling. In that respect Eq. (4.7) is consistent with the phenomenological stress-growth law proposed by Fung and shown schematically in Fig. 7. It is assumed the time course of graft dissolution parallels that kinetics of the regenerative arterial thickening, so that

$$H_g(t) = H_g^0 - H_a(t) \tag{4.8}$$

where H_g^0 and $H_g(t)$ are the initial and the current thickness of the graft, respectively.

To model phenomenologically the processes leading to an increase in stiffness of the neo-arterial tissue, it is hypothesized that the neo-artery alters its mechanical properties to restore the baseline value of the pulsatile circumferential strain due to the variation of the pressure from its diastolic to systolic value. Similar hypothesis was proposed to model mechanical remodeling of

healthy arteries subjected to sustained hypertension [44]. The parameter that relates a small variation in the circumferential strain and small variation in distending pressure of a long cylindrical tube is called the compliance. By definition it is given by the relation

$$C = \frac{\Delta r}{r \Delta P} \tag{4.9}$$

where Δr is the small variation of the mid-wall radius r due to the variation of the pressure by ΔP. Compliance characterizes the overall deformability of a tube. It is calculated by considering the small axisymmetric radial deformation superposed on the known finite deformed state. The ratio $e = \Delta r/r$ is analogous to the classical infinitesimal strain. It represents the relative increase in the mid-wall circumference with respect to the finitely deformed configuration. Given the pressure variation ΔP, the strain e is proportional to compliance C. In keeping with the introduced hypothesis the evolution equation for the material constant A_a is postulated in the form

$$\frac{dA_a(t)}{dt} = \begin{cases} \frac{1}{T_1} \frac{k_1 C_0 - C}{C_0} & \text{if } C < k_1 C_0, \\ 0 & \text{if } k_1 C_0 < C < k_2 C_0, \\ \frac{1}{T_2} \frac{C - k_2 C_0}{C_0} & \text{if } C > k_2 C_0. \end{cases} \tag{4.10}$$

C is the current compliance of the artery/graft complex calculated at the mid-wall radius of the neo-artery; C_0 is the baseline value of the arterial compliance. The coefficients $k_1 \leqslant 1$ and $k_2 \geqslant 1$ specify the threshold values of the compliance mismatch, which can elicit changes in the mechanical properties, T_1 and T_2 are rate constants. According to Eq. (4.10) the arterial material increases its stiffness in response to an abnormal pulsatile strain of the arterial wall estimated through the deviation of the current arterial compliance from its baseline value. Equation (4.10) is in agreement with the experimental observations that cyclic overstretching as well as loss of stretch experienced by the smooth muscle cells provokes their synthetic and proliferative activity [67]. Increased production of collagen and extracellular matrix ultimately leads to a change in the mechanical properties of the arterial tissue.

Thus, formation of a neo-artery is described by a system of two nonlinear first order differential equations, (4.7) and (4.10), for the evolution of the arterial geometry and mechanical properties. These equations are coupled to the equation of equilibrium and to the equations describing the changes

in the geometry and mechanical properties of the resorbable prosthesis, (4.6) and (4.8).

4.3.3. Results and Discussion. The dimensions and the mechanical properties of vessel material were specified for a aorta and a resorbable graft taken from the literature [65, 66]. The model parameters were chosen to yield a reasonable time course of the regeneration and resorption processes. The governing equations were solved numerically using an explicit time step. The material constants of the graft material, the stress distribution and the compliance of the artery/graft complex are calculated at each time step. The values of the mean arterial stress and the compliance are substituted into the evolution equations and the new thickness and elastic constants of neo-artery are calculated. The procedure is repeated and terminated, provided it is self-limiting, when the graft thickness vanishes and the dimensions and mechanical properties of the neo-artery attain values close to those of a normal artery.

The time course of the arterial thickness exhibits a N-shaped pattern (Fig. 19a), similar to the experimental observations in [61] for regeneration of a rabbit aorta over a bioresorbable PGA (polyglicolic acid) graft, (Fig. 17). Material constants of arterial tissue monotonically increase attaining the values of a normal artery (Fig. 19b), while the graft constants decrease following the prescribed linear dependence on time (not shown).

The stress experienced by the artery, (Fig. 19c), is compressive in the early stage of graft resorption as it was found in the linear study [62]. When the grafts resorbs, but the neo-artery has not gained sufficient thickness and stiffness, the circumferential arterial stress increases and takes values higher than the "equilibrium" physiological stress. Due to progressive thickening of the artery the stress decreases and reverts to a value close to the stress in the native artery. The time course of the compliance that drives the stiffening of the neo-arterial material has non-monotonic pattern (Fig. 19d).

A parametric study was performed varying the thickness, stiffness and rate of mechanical softening of the bioresorbable grafts. It was shown that fast resorption of the graft material leads to overloading of the neo-artery tissue before it is sufficiently organized to bear load. This might lead to bursting or aneurismal dilatation, as had been experimentally observed [61, 68]. Similar effects are theoretically predicted when the graft exhibits a small initial wall thickness (Fig. 19c)

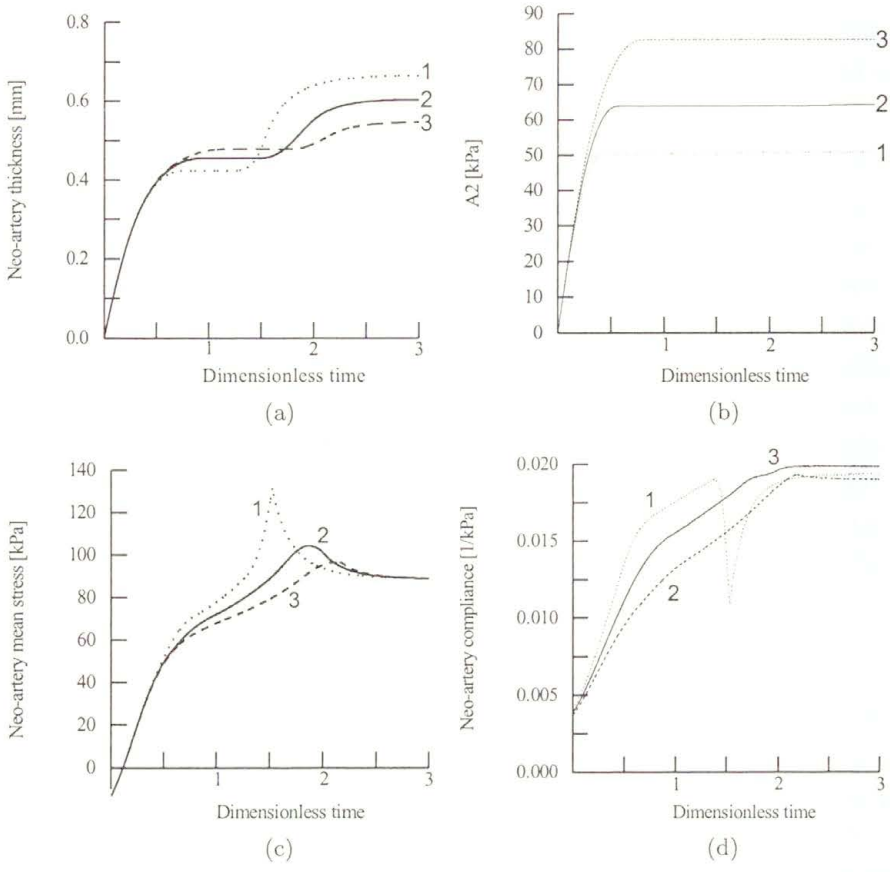

FIGURE 19. Predicted time course of: (a) neo-artery wall thickness; (b) neo-artery material constant A_2; (c) mean circumferential stress in the neo-arterial wall; (d) compliance of the neo-artery/graft complex. The initial graft thickness is 0.50 mm; (curves '1'), 0.60 mm (curves '2') and 0.65 mm (curves '3').

In conclusion, the results obtained support the hypothesis that arterial regeneration over a bioresorbable graft is an adaptive process and is influenced and modulated by mechanical factors. If the mean circumferential stress and pulsatile stretch are accepted as major determinants of the vessel wall regeneration, the process is self-limiting and leads to formation of a vessel with dimensions and mechanical properties close to those of a normal artery. Prostheses that slowly resorb and have sufficient wall thickness might more reliably allow for development of a neo-artery of adequate strength necessary to prevent bursting or aneurismal dilatation.

More experimental studies are needed to verify the introduced hypothesis and to identify all model parameters and functions. It is necessary to specify

a reliable parameter, or group of parameters, that allow describing the time variation of the mechanical properties of the neo-arterial tissue and the resorbable graft. Comparison of model predictions with experimental data will promote testing the introduced hypotheses and refining the model. Further generalization of the model should account for the development of residual strains and stresses in the neo-artery originating from volumetric remodeling. After experimental validation the model predictions can be used for improvement of graft design and selection. The simple model proposed in this study was aimed to focus on such a possibility and to provoke further investigations.

5. Appendices

Use of solid mechanics for a strain and stress analysis of an artery requires adoption of a relevant mathematical model. Modeling includes: i) assumptions for arterial geometry (geometrical model); ii) assumptions for the interaction of the vessel with other bodies (model of loading and boundary conditions); iii) mathematical description of the mechanical properties of the vascular tissue (selection of constitutive equations); and iv) assumptions concerning the deformation process by introducing hypotheses for the character of the strain and/or stress state in the arterial wall. Depending on geometrical dimensions of a specific artery and on the objectives of the investigation, the blood vessel might be considered as a three- or as a two-dimensional body.

A. 3-D Stress and Strain Analysis of Arteries

As have been demonstrated in several studies, [69, 70], a radial cut on a unloaded arterial segment makes it spring open and the cross-section takes a shape close to a circular sector (Fig. 20(a)). Assuming that in this configuration the vessel is in the zero-stresses state, the cut-opened configuration is used as a reference configuration to define strains. The angle Φ, called the *opening angle*, was introduced by Chuong and Fung [69]. It is an indicator for existence of residual stresses and strains in the state of no load.

Under physiological conditions an artery is subjected to internal pressure and is extended in the axial direction. It undergoes an axisymmetric finite deformation from the zero-stress configuration to the deformed configuration,

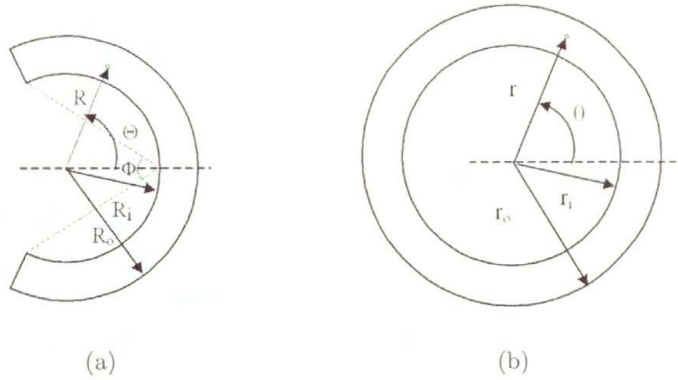

FIGURE 20. Schematic representation of the arterial cross-section (a) at the zero-stress state and (b) at the current deformed state

which is considered to be a circular thick-walled tube in the state of plane strain (Fig. 20(b)).

The arterial tissue is assumed to be an orthotropic incompressible elastic material, with axes of orthotropy in the radial, circumferential and longitudinal directions. The constitutive equations follow from a strain energy density function (SEF) that is a function of the principal strains.

Given the dimensions at the zero-stress state, SEF, the internal pressure, and the axial stretch ratio (or the total axial force), the strain and stress distribution in the arterial wall is determined using a semi-inverse method. The deformation from the zero-stress state to the current deformed state is prescribed in terms of relations that contain a finite number of unknown deformation parameters. After having calculated the strain and stress field, the deformation parameters are determined from the equations of equilibrium and the boundary conditions.

Using the notation given in Fig. 20, the deformation is described by the relations

$$\mu = \frac{r_i}{R_i}, \quad \chi = \frac{\pi}{\pi - \Phi}, \quad \lambda = \frac{l}{L} \tag{A.1}$$

where μ, χ and λ are deformation parameters; l and L are the length of the arterial segment at the zero-stress state and at the deformed state, respectively.

Following the theory of finite deformations, [24], and denoting the cylindrical coordinates of an arbitrary point before and after deformation by (R, Θ, Z) and (r, θ, z), the stretch ratios in the radial, circumferential and

axial direction are

$$\lambda_r = \frac{dr}{dR}, \quad \lambda_\theta = \frac{\pi r}{(\pi - \Phi)R} = \chi \frac{r}{R}, \quad \lambda_z = \lambda. \tag{A.2}$$

The principal components of Green strain are

$$e_i = \frac{1}{2}(\lambda_i^2 - 1), \quad i = r, \theta, z. \tag{A.3}$$

It follows from the incompressibility of the material that $\lambda_r \lambda_\theta \lambda_z = 1$ and hence

$$\frac{dr}{dR}\frac{r}{R}\chi\lambda = 1. \tag{A.4}$$

After integrating Eq. (A.4)

$$r = \sqrt{\frac{R^2}{\chi\lambda} + R_i^2 \left(\mu^2 - \frac{1}{\chi\lambda}\right)}. \tag{A.5}$$

The strain energy function can be given in two alternative forms. If $W = W(e_r, e_\theta, e_z)$ the constitutive relations between the principal Cauchy stress and Green strains are

$$\sigma_r = \lambda_r^2 \frac{\partial W}{\partial e_r} + p, \quad \sigma_\theta = \lambda_\theta^2 \frac{\partial W}{\partial e_\theta} + p, \quad \sigma_z = \lambda_z^2 \frac{\partial W}{\partial e_z} + p \tag{A.6}$$

where p is unknown scalar function, which appears due to the material incompressibility.

If the condition of incompressibility is used to eliminate the radial strain e_r then $\tilde{W} = \tilde{W}(e_\theta, e_z)$ and the constitutive equations are

$$\sigma_\theta = \lambda_\theta^2 \frac{\partial \tilde{W}}{\partial e_\theta} + \sigma_r, \quad \sigma_z = \lambda_z^2 \frac{\partial \tilde{W}}{\partial e_z} + \sigma_r. \tag{A.7}$$

Both the formulations of the constitutive equations given by Eqs. (A.6) and (A.7) are three-dimensional.

Equations of equilibrium yield

$$\frac{d\sigma_r}{dr} + \frac{\sigma_r - \sigma_\theta}{r} = 0, \quad \frac{\partial p}{\partial \theta} = 0, \quad \frac{\partial p}{\partial z} = 0. \tag{A.8}$$

Integrating Eqs. (A.8) and using the boundary condition at the inner cylindrical surface $\sigma_r(r = r_i) = -P$, where P is the applied pressure, the

principal stresses are

$$\sigma_r = \int_{r_i}^{r} \left(\lambda_\theta^2 \frac{\partial W}{\partial e_\theta} - \lambda_r^2 \frac{\partial W}{\partial e_r} \right) \frac{dr}{r} - P,$$
$$\sigma_\theta = \sigma_r + \lambda_\theta^2 \frac{\partial W}{\partial e_\theta} - \lambda_r^2 \frac{\partial W}{\partial e_r}, \tag{A.9}$$
$$\sigma_z = \sigma_r + \lambda_z^2 \frac{\partial W}{\partial e_z} - \lambda_r^2 \frac{\partial W}{\partial e_r}.$$

Given the opening angle the parameter χ is known. The remaining deformation parameters μ and λ are determined from the condition that the outer cylindrical surface is traction free, $\sigma_r\,(r = r_0) = 0$, and from the condition that the axial force F applied to the vessel is given

$$P = \int_{r_i}^{r_o} \left(\lambda_\theta^2 \frac{\partial W}{\partial e_\theta} - \lambda_r^2 \frac{\partial W}{\partial e_r} \right) \frac{dr}{r}, \quad F = 2\pi \int_{r_i}^{r_o} \sigma_z r dr. \tag{A.10}$$

If the axial stretch ratio λ instead of force F is given, the only unknown parameter μ is calculated using Eq. $(A.10)_1$. Having determined the deformation parameters, the strain and stress distributions in the arterial wall are calculated using Eqs. (A.5), (A.2), (A.4) and (A.9). When the strain energy function is given in the form $\tilde{W} = \tilde{W}(e_\theta, e_z)$ the Eqs. (A.9) and (A.10) are modified accordingly by setting the derivatives with respect to e_r equal to zero and replacing W by $\tilde{W}$.

In the particular case of an unloaded arterial segment the unknown deformation parameters μ and λ are to be determined from the Eqs. (A.10) by setting $P = 0$ and $F = 0$. Calculations have shown that with a good accuracy the value of the deformation parameter λ is close to 1 as it was set in [69]. The strains and stresses corresponding to the state of no load are called the *residual strains and stresses*. Because no load is applied, the residual stresses are equilibrated in the artery wall. They are compressive at a portion of the wall thickness close to the inner surface and are tensile in a portion of the wall close to the outer surface. When a thick-walled tube is subjected to an internal pressure the circumferential stress is higher at the inner surface. Existence of residual strains reduces the strain gradient across the arterial wall under physiological load conditions and leads to optimal, from a mechanical point of view, bearing of applied load by the structural elements of media [69]. Moreover, a close to uniform distribution of the circumferential

strain and stress provides a uniform local mechanical environment for vascular smooth muscle cells throughout the arterial wall and thus optimizes their performance. Evidently there exist no residual strains if the opening angle is zero.

The analysis given above was generalized for the case when an artery is considered to be a two-layered tube [71]. The field equations were written for each layer and conditions for continuity of the radial displacement and the radial stress were imposed. Given that the axial stretch ratio is the same in both layers, the stress and strain fields again depend on a single deformation parameter, which is determined form an equation similar to Eq. $(A.10)_1$ but the integration is performed over the thickness of both the layers.

To account for the contribution of the vascular smooth muscle the described analysis was modified in two directions [46]. First, the opened-up configuration when the smooth muscle cells are maximally relaxed was taken to be a zero-stress reference state. Secondly, the circumferential stress was represented as a sum of a stress calculated from the constitutive equations (A.7) or (A.8) and termed as passive stress; and an active circumferential stress developed by the stimulated smooth muscle (see Eq. 3.10).

B. 2D-Stress and Strain Analysis of Arteries

In some cases an artery can be considered as a thin-walled circular cylindrical *membrane* of constant thickness. Its deformed state is described by the deformation of the mid-wall surface. The stresses acting in cross-sections normal to the middle surface are assumed uniformly distributed across the thickness, while the stresses in cross-sections parallel to the middle surface are assumed to be zero. Stress and strain analysis based on the three-dimensional consideration has shown that the membrane approach is asymptotically valid provided the following conditions hold true: i) the thickness is sufficiently smaller compared to the other dimensions of the membrane; in particular for circular cylindrical membranes the thickness to radius ratio has to be less than 0.2; ii) the radius, thickness, mechanical properties, and applied load vary in a smooth manner along the membrane surface; iii) the boundary conditions do not impose restrictions on the deformations of the middle surface. These conditions are satisfied for healthy non-stenosed aorta and large arteries subjected to physiological loads and located far away from bifurcations.

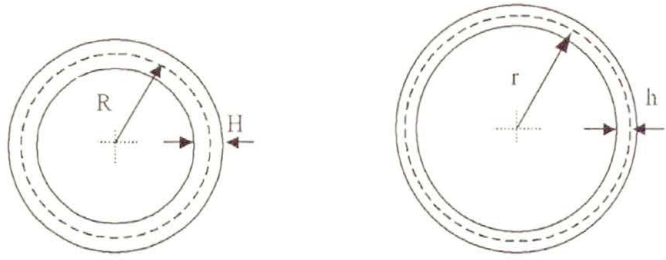

FIGURE 21. Schematic representation of the arterial cross-section (a) at the zero-stress state and (b) at the current deformed state.

The state of no load is taken as a reference state to calculate the strain components (Fig. 21).

When the membrane is inflated by an internal pressure and is extended longitudinally it undergoes an axisymmetric finite deformation (Fig. 21b). The membrane stretch ratios in the axial and circumferential directions are

$$\lambda_z = \frac{l}{L}, \quad \lambda_\theta = \frac{r_m}{R_m}, \tag{B.1}$$

where R_m and r_m are the mid-wall radii of the artery at the unloaded and deformed state respectively, and L and l are the corresponding axial lengths. It follows from the condition of incompressibility that

$$\lambda_r = \frac{h}{H} = \frac{1}{\lambda_z \lambda_\theta} \tag{B.2}$$

where h and H is the deformed and undeformed wall thickness, respectively. The Green strains are given again by Eq. (A.3).

The membrane circumferential and the axial stress are uniformly distributed across the wall thickness, while the radial stress is zero everywhere. Depending on the form in which the membrane strain energy density function is given the constitutive equations are

$$\sigma_\theta = \lambda_\theta^2 \frac{\partial W_m}{\partial e_\theta} - \lambda_r^2 \frac{\partial W_m}{\partial e_r}, \quad \sigma_z = \lambda_z^2 \frac{\partial W_m}{\partial e_z} - \lambda_r^2 \frac{\partial W_m}{\partial e_r} \tag{B.3}$$

if the strain energy function is given in the form $W_m = W_m(e_r, e_\theta, e_z)$, or

$$\sigma_\theta = \lambda_\theta^2 \frac{\partial \tilde{W}_m}{\partial e_\theta}, \quad \sigma_z = \lambda_z^2 \frac{\partial \tilde{W}_m}{\partial e_z} \tag{B.4}$$

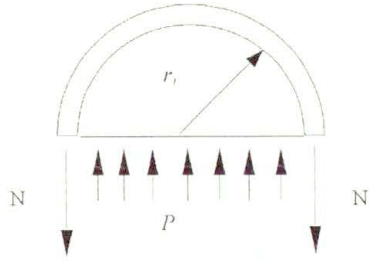

FIGURE 22. Free body diagram of an artery

if the strain energy function is given in the form $\tilde{W}_m = \tilde{W}_m(e_\theta, e_z)$. Both formulations are two-dimensional. It is worth noting that the membrane strain energy functions W_m and $\tilde{W}_m$ are functions of the strains calculated for the middle surface, and are in general different than the three-dimensional strain energy functions W and $\tilde{W}$.

Because the stresses are uniformly distributed across the wall thickness their stress resultants, called the *membrane tensions*, are

$$N_\theta = h\sigma_\theta, \quad N_z = h\sigma_z. \tag{B.5}$$

The equation of the overall equilibrium in the radial direction (Fig. 22) yields $\sigma_\theta = Pr_i/h$, a formula known as *law of Laplace*. Using Eqs. (B.1) and (B.2), it takes the form

$$\sigma_\theta - P\left[\frac{\lambda_z \lambda_\theta^2 R}{H} - \frac{1}{2}\right] = 0. \tag{B.6}$$

Given the zero-stress configuration, the strain energy function, the axial stretch ratio λ_z and the applied pressure, the unknown stretch ratio λ_θ is determined from Eq. (B.6) and all membrane stresses and strains can be calculated. It is evident from Eq. (B.6) that the membrane approach implies that the unloaded membrane is in the stress-free state.

The membrane approach is simpler than the more general 3-D consideration. However, it does not allow determining the strain and stress distribution across the wall thickness and disregards the existence of radial stress. Moreover, the membrane consideration neglects the effects of the residual strains. Therefore, it excludes a comparison between theoretically predicted values of the opening angle and its experimental records to be used as a tool for validating models of arterial remodeling and growth.

A systematic and comprehensive description of arterial wall mechanics and a comparative study of most material models are given by Holzapfel et al. in [72].

References

1. A.V. HILL, *The heat of shortening and the dynamic constants of muscle*, Proc. Roy. Soc. London Ser. B, **126**: 136–195, 1939.

2. L.A. TABER, *Biomechanics of growth, remodeling, and morphogenesis*, Appl. Mech. Rev., **48**: 489–545, 1995.

3. J.D. HUMPHREY, *Cardiovascular solid mechanics: cells, tissues, and organs*, Springer-Verlag, New York Berlin Heiderberg 2002.

4. W. ROUX, *Der zuchtende Kampf der Teile (Theorie der funktionellen Anpassung)*, In W. Engelmann, (ed.), Gesammelte Abhandlungen uber die Entwicklungsmechanik der Organismen, **1**: 137–422, 1885.

5. R. THOMA, *Untersuchungen uber die Histogenese und Histomechanik des Gefassystems*, Enke, Stuttgart 1893.

6. Y.C. FUNG, *Biomechanics. Motion, Flow, Stress and Growth*, Springer-Verlag, New York 1990.

7. A.A. STEIN, *Application of continuum mechanics methods to the modeling of growth of biological tissues*, In L.V. Beloussov, and A.A. Stein (eds.), Mechanics of growth and morphologenesis, pp.148–173, Moscow University press, Moscow 2000.

8. T. MATSUMOTO, M. TSUCHIDA AND M. SATO, *Change in intramural strain distribution in rat aorta due to smooth muscle contraction and relaxation*, Am. J. Phys., **271**: 1711–1716, 1996.

9. A. KAMIYA and T. TOGAWA, *Adaptive regulation of wall shear stress to flow change in canine carotid artery*, Am. J. Phys., **239**: 14–21, 1980.

10. B.L. LANGILLE, M.P. BENDECK and W. KEELEY, *Adaptations of carotid arteries of young and mature rabbits to reduced carotid blood flow*, Am. J. Physiol., **256**: 931–939, 1989.

11. R.D BROWNLEE and B.L LANGILLE, *Arterial adaptation to altered blood flow*, Canad. J. Physiol. Pharm., **69**: 978–983, 1991.

12. B.L. LANGILLE, *Blood flow-induced remodeling of the artery wall*, In J.A. Bevan, G. Kaley and G. Rubanyi (eds.), Flow-dependent regulation of vascular function, pp.227–299, American Society of Mechanical Engineers, New York, Oxford 1995.

13. J.E. HASSON, J. MEGERMAN, and W.M. ABBOTT, *Increased compliance near vascular anastomoses*, J. Vasc. Surg., **2**: 419–423, 1985.

14. M. ZAMIR, *Shear forces and blood vessels radii in the cardiovascular system*, Journal of General Physiology, **69**: 449–461, 1979.

15. L.A. TABER, S. NG, A.M. QUESNEL, J. WHATMAN, and C. J. CARMEN, *Investigating Murray's law in the chick embryo*, J. Biomech., **34**: 121–124, 2001.

16. Y.C. FUNG, *Biomechanics. Circulation*, 2nd ed., Springer-Verlag, New York–Berlin–Heidelberg 1996.

17. H. MASUDA, H. BASSIOUNY, S. GLAGOV, and C.K. ZARINS, *Artery wall restructuring in response to increased flow*, Surg. Forum, **40**: 285–286, 1989.

18. S. GLAGOV, C.K ZARNIS, N. MASAWA, C.P. XU, H. BASSIOUNY and D.P. GIDDENS, *Mechanical functional role of non-atherosclerotic intimal thickening*, Frontiers Med. Biol. Eng., **1**: 37–43, 1993.

19. B.L. LANGILLE, *Remodeling of developing and mature arteries: Endothelium, smooth muscle and matrix*, J. Cardiovasc. Pharmacol., **21**(Suppl. 1): 11–17, 1993

20. W. FATH, H.M. BURKHART, S.C. MILLER, M.C. DALSHING, and J.L. UNTHANK, *Wall remodeling after wall shear rate normalization in rat mesenteric collaterals*, J. Vasc. Res., **35**: 257–264, 1998.

21. B.L. LANGILLE and F. O'DONNELL, *Reductions in arterial diameter produced by chronic decrease in blood flow are endothelium-dependent*, Science Wash. DC, **231**: 405–407, 1986.

22. S.Q. LIU and Y.C. FUNG, *Relationship between hypertension, hypertrophy and opening angle of zero-stress state of arteries following aortic constriction*, J. Biomech. Engr., **111**:325–335, 1989.

23. Y.C. FUNG and S.Q. LIU, *Change of residual strains in arteries due to hypertrophy caused by aortic constriction*, Circ. Res., *65*:1340–1349, 1989.

24. A.E. GREEN, AND J.E. ADKINS, *Large Elastic Deformations and Nonlinear Continuum Mechanics*, Oxford University Press, London 1970.

25. R.N. VAISHNAV, J. VOSSOUGH, D.J. PATEL, I.N COTHRAN, B.R. COLEMAN, and E.L. ISON-FRANKLIN, *Effect of hypertension on elasticity and geometry of aortic tissue from dogs*, J. Biomech. Engr., **112**:70–74, 1990.

26. T. MATSUMOTO AND K. HAYASHI, *Mechanical and dimensional adaptation of rat aorta to hypertension*, J. Biomech. Engr., **116**:278–283, 1994.

27. C.L. BERRY and S.E. GREENWALD, *Effects of hypertension on the static mechanical properties and chemical composition of rat aorta*, Cardiovasc. Res., **10**:437–451, 1976.

28. P. FRIDEZ, A. MAKINO, H. MIYAZAKI, J.-J. MEISTER, K. HAYASHI and N. STERGIOPULOS, *Short-term biomechanical adaptation of the rat carotid to acute hypertension: contribution of smooth muscle*, Ann. Biomed. Engr., **29**(1) 26–34, 2001.

29. K. HAYASHI, A. MAKINO, D. KAKOI, and H. MIYAZAKI, *Remodeling of arterial wall in response to blood pressure and blood flow changes*, Proceeding of 2001 Summer Bioengineering Conference, pp.819–820, 2001.

30. T. MATSUMOTO, E. OKUMURA, Y. MIURA, and M. SATO, *Mechanical and dimensional adaptation on rabbit carotid artery cultured in vitro*, Med. Biol. Eng. Comput., **37**:252–256, 1999.

31. H.-C. HAN and D.N. KU, *Contractile response of arteries subjected to hypertensive pressure in seven-day organ culture*, Ann. Biomed. Engr., **29**:467–475, 2001.

32. H.-C. HAN, R.P. VITO, K. MICHEAL and D.N. KU, *Axial stretch increases cell proliferation in arteries in organ culture*, Advances in Bioengineering, ASME, **48**: 63–64, 2000.

33. D.Y.M. LEUNG, S.G. GLAGOV and M.B. MATHEWS, *Cycling stretching stimulates synthesis of components by arterial smooth muscle cells in vivo*, Science, **116**: 455–477, 1976.

34. R. NEREM, *Hemodynamics and the vascular endothelium*, J. Biomech. Engr., **115**: 510–514, 1993.

35. A. KAMIYA and J. ANDO, *Response of vascular endothelial cells to fluid shear stresses: Mechanism*, In K. Hayashi, A. Kamiya, and K. Ono (eds.), Biomechanics, Functional Adaptation and Remodeling, Springer-Verlag, Tokyo 1996.

36. R. SKALAK, *Growth as finite displacement field*, In D.E. Carlson, R.T. Shield (eds.), Proceedings of the IUTAM Symposium on finite elasticity, pp.347-355, Martinus Nijhoff, The Hage 1981.

37. E.K. RODRIGUEZ, A. HOGER, and A.D. MCCULLOCH, *Stress-dependent finite growth in soft elastic tissues*, J. Biomech., **27**: 455–467, 1994.

38. L.A. TABER, *A model for aortic growth based on fluid shear and fiber stresses*, J. Biomech., **120**: 348–354, 1998.

39. J.D. HUMPHREY and K.R. RAJAGOPAL, *A constrained mixture model for arterial adaptations to sustained step change in blood flow*, Biomech. Model Mechnobiol., **2**: 109–126, 2003.

40. Y.C. FUNG, *What are the residual stresses doing in our blood vessels?*, Ann. Biomed. Engr., **19**: 237–249, 1991.

41. L.A. TABER and D.W. EGGERS, *Theoretical study of stress-modulated growth in the aorta*, J. Theoret. Biol., **180**: 343–357, 1996.

42. L.A. TABER, *Biomechanical growth laws for muscle tissue*, J. Theoret. Biol., **193**(2): 201–213, 1998.

43. A. RACHEV, N. STERGIOPULOS, and J.-J. MEISTER, *Theoretical study of dynamics of arterial wall remodeling in response to changes in blood pressure*, J. Biomech., **5**: 635–642, 1996.

44. A. RACHEV, N. STERGIOPULOS, and J.-J. MEISTER, *A model for geometrical and mechanical adaptation of arteries to sustained hypertension*, J. Biomech. Engr., **120**:9–17, 1998.

45. A. RACHEV, *A model of arterial adaptation to alterations in blood flow*, J. Elasticity, **61**(1/3):83–111, 2000.

46. A. RACHEV AND K. HAYASHI, *Theoretical study of the effects of vascular smooth muscle contraction on strain and stress distributions in arteries*, Ann. Biomed. Engr., **27**:459–468, 1999.

47. C. REMBOLD AND R. MURPHY, *Latch-bridge model in smooth muscle: $[Ca^{2+}]$ can quantitatively predict stress*, Am. J. Physiol., **259**:251–259, 1990.

48. P.B. DOBRIN, *Influence of initial length on length-tension relationship of vascular smooth muscle*, Am. J. Physiol., **225**:659–663, 1973.

49. A. RACHEV, TZ. IVANOV, and K. BOEV, *A model for contraction of smooth muscle (translated from Russian)*, Mech. Comp. Mat., **2**:259–263, 1980.

50. H. ACHAKRI, A. RACHEV, N. STERGIOPULOS, and J.-J. MEISTER, *A theoretical investigation of low frequency diameter oscillations of muscular arteries*, Ann. Biomed. Engr., **22**:253–263, 1994.

51. S. RODBARD, *Negative feedback mechanisms in the architecture and function of the connective and cardiovascular tissue*, Perspectives in Biology and Medicine, **13**:507–527, 1970.

52. N. STERGIOPULOS, *Using hemodynamics to limit stent restenosis rates: the ARES stent principle*, In 12th Conference of the European Society of Biomechanics, p.302, 2000.

53. R. HOFFMAN, G.S. MINTZ, G.R. DUSSAILLANT, J.J. POPMA, A.D. PICHARD, L.F SATLER, K.M. KENT, J. GRIFFINN, and M.B. LEON, *Patterns and mechanisms of in-stent restenosis a serial intravascular ultrasound study*, Circulation, **94**:1247–1254, 1996.

54. J.A. DEWEESE, *Anastomotic neointimal fibrous hyperplasia*, In V.M. Brenhard and J.B. Towne (eds.), *Complications in vascular surgery*, pp.157–170, Grune and Stratton, Orlando 1985.

55. V. ECHAVE, A.R. KOORNICK, M. HAIMOV and J.H. JACOBSON, *Intimal hyperplasia as a complication of the use of the polytetrafluoroethylene graft for femoral-popliteal bypass*, Surgery, **86**: 791–798, 1979.

56. P.E. PAASCHE, C.E KINLEY, F.G. DOLAN, E.R. GONAZ and A.E MARBLE, *Consideration of suture line stresses in the selection of synthetic grafts for implantation*, J. Biomech., **6**: 253–259, 1973.

57. K.B. CHANDRAN, D. GAO, G. HAN, H. BARANIEWSKI, and J.D. CORSON, *Finite-element analysis of arterial anastomoses with vein, dacron and PTFE grafts*, Med. Biol. Eng. Comput., **30**: 413–418, 1992.

58. T. MATSUMOTO, H. ITAGAKI, and K. HAYASHI, *FEM analysis of stress and deformation in vicinities of arterial graft anastomosis*, Journal of Applied Biomaterials, **5**: 79–87, 1994.

59. A. RACHEV, E. MANOACH J. MOORE JR., and J. BERRY, *A model of stress-induced geometrical remodeling of vessel segments adjacent to stents and artery/graft anastomoses*, J. Theoret. Biol., **206**: 429–443, 2000.

60. J.E. HASSON, J. MEGERMAN, and W. M. ABBOTT, *Increased compliance near vascular anastomoses*, J. Vasc. Surg., **2**: 419–423, 1985.

61. H. GREISLER, J. ELLINGER, T. SCHWARCZ, A. GOLAN, R. RAYMOND, and D. KIM, *Arterial regeneration over polydioxanone prostheses in the rabbit*, Arch. Surg., **122**: 715–721, 1987.

62. D. VORP, M. RAGHAVAN, H. BOROVETZ, H. GREISLER, and M. WEBSTER, *Modeling the transmural stress distribution during healing of bioresorbable vascular prostheses*, Ann. Biomed. Engr., **23**: 178–188, 1995.

63. A. RACHEV and M. KIRILOVA, *A mathematical model of arterial regeneration over bioresorbable grafts*, Proc. of Fourth World Congress of Biomechanics, Calgary 2002.

64. M. KIRILOVA and A. RACHEV, *A theoretical investigation of the effects of bioresorbable material on process of neo-artery regeneration*, Proc. of the 9-th National Congress of Theoretical and Applied Mechanics, 19-22 IX 2001, Varna, **II**: 159–164, 2004.

65. S. STEWART and D. LYMAN, *Finite elasticity modeling the biaxial and uniaxial properties of compliant vascular grafts*, J. Biomech. Engr., **110**: 344–348, 1988.

66. D.J. PATEL and R.N. VAISHNAV, *The rheology of large blood vessels*, In: Cardiovascular Fluid Dynamics, **2**: 1–64, Academic, New York 1972.

67. S. LEHOUX and A. TEDGUI, *Signal transduction of mechanical stresses in the vascular wall*, Hypertension, **32**: 338–345, 1998.

68. H. GREISLER, E. ENDEAN, J. KLOSAK, J. ELLINGER, J. DENNIS, K. BUTTLE, and D. KIM, *Polyglactin 910/polydioxanone bicomponent totally resorbable vascular prostheses*, J. Vasc. Surg., **7**: 697–705, 1988.

69. C.J. CHUONG and Y.C. FUNG, *On residual stress in arteries*, J. Biomech. Eng., **108**: 189–192, 1986.

70. R.N. VAISHNAV and J. VOSSOUGHI, *Estimation of residual strains in aortic segments*, In C.W. Hall (ed.), Biomedical Engineering II: Recent Developments, pp.330–333, Pergamon Press, New York 1983.

71. A. RACHEV, *Theoretical study of the effect of stress-dependent remodeling on arterial geometry under hypertensive conditions*, J. Biomech., **8**: 819–827, 1997.

72. G.A. HOLZAPFEL, T.C. GASSER and R.W. OGDEN, *A new constitutive framework for arterial wall mechanics and a comparative study of material models*, J. Elasticity, **61**: 1–48, 2000.